GEOLOGICKÝ ZBORNÍK — GEOLOGICA CARPATHICA, 39, 4, BRATISLAVA, AUGUST, 1988,
Pp. 455—488

MARIAN JANÁK* — ŠTEFAN KAHAN** — DUŠAN JANČULA***

METAMORPHISM OF PELITIC ROCKS AND METAMORPHIC ZONES IN SW PART OF WESTERN TATRA MTS. CRYSTALLINE COMPLEXES

(Figs. 14, Tabs. 6)

Abstract: Progressive increase of metamorphic conditions in the SW part of the Western Tatra Mts. crystalline complexes caused the formation of metamorphic zones — staurolite-kyanite-sillimanite zone and sillimanite zone divided into subzones 1 and 2. The metamorphic zoning was the result of regional metamorphism, most probably in the Hercynian cycle. The Hercynian granitoid body is surrounded by migmatites and metamorphites of the highest-temperature sillimanite zone 2, where partial anatexis took place. Space distribution of the metamorphic zones was affected as well by tectonic processes, especially by thrusting of the crystalline complexes.

Progressive increase of P-T-X conditions caused changes in the mineral assemblages of the metapelites as well as in the composition of the individual studied minerals. The transition from the staurolite-kyanite-sillimanite zone into the sillimanite zone is expressed by the isograd of staurolite breakdown with sillimanite formation. The formation of sillimanite occurred as a result of decomposition reactions of staurolite, kyanite, biotite, garnet and muscovite. The coexistence of kyanite and sillimanite is discussed from the viewpoint of their mutual stability which corresponded to P-T conditions near the curve of their univariant equilibrium.

P-T conditions of progressive metamorphism determined on the basis of thermobarometry and petrogenetic grid corresponded to temperatures of 530—700 °C at pressures of 4—7 kbar and an assumed fluid phase composition with $X_{H_2O} \approx 0.8$; this corresponds to the medium-pressure type of the kyanite-sillimanite type of facies series. In connection with the effects of fluids at lower P-T conditions retrograde alterations took place with the formation of especially chloritoid, chlorite and white micas (muscovite and margarite).

Резюме: Прогрессивный возраст метаморфических условий в ЮЗ части кристаллиникума Западных Татер вызвал образование метаморфических зон — ставролит-кианит силлиманитовой и силлиманитовой разделенной на субзоны 1 и 2. Метаморфическая зональность является результатом регионального метаморфизма, правдеподобно в Герцинском цикле. Герцинское гранитоидное тело окружено мигматитами и метаморфическими породами наиболее высокотемпературной силлиманитовой зоны 2, где были достигнуты условия парциального анатексиса. На пространственное распределение метаморфических зон оказали влияние тоже тектонические процессы, прежде всего перемещение частей кристаллиникума.

---

* RNDr. M. Janák, Department of Mineralogy and Petrology, Fac. of Natural Sci., Comenius University, Mlynská dolina, B-2, 842 15 Bratislava.

** Doc. RNDr. Š. Kahan, CSc., Department of Geology and Paleontology Fac. of Natural Sci., Comenius University, Mlynská dolina, B-2, 842 15 Bratislava.

*** RNDr. D. Jančula, Central Laboratory of Chemical Technics, Slovak Institute of Technology, Radlinského 9, 812 37 Bratislava.

Прогрессивный возраст P-T-X условый вызвал изменения в минеральных ассоциациях и в составе отдельных изучаемых минералов. Переход от ставролит-кианит-силлиманитовой зоны к силлиманитовой зоне выражен изоградой распада ставролита при образовании силлимнита. Образование силлиманита было результатом реакций распада ставролита, кианита, биотита, граната и мусковита. Сосуществование кианита и силлиманита дискутируется с точки зрения их взаимной устойчивости соответствующей P-T условиям близ кривой их унивариантного равновесия.

P-T условия прогрессивного метаморфизма определенные на основе термобарометрии и петрогенетической сетки соответствовали температурам 530—700 °C при давлении 4—7 kbar и предполагаемом составе флюидной фазы с $X_{H_2O} \approx 0{,}8$; это соответствует среднеглубинному типу кианит-силлиманитого метаморфизма. В связи с воздействием флюидов при низших P-T условиях появились ретроградные изменения при образовании хлоритоида, мусковита и маргарита.

Introduction

The latest works concerning the crystalline complexes of the Western and High Tatra Mts. on Czechoslovak territory (Gorek, 1956, 1959, 1967, 1969; Kahan, 1967, 1968, 1969) as well as on Polish territory (Jaroszewski, 1965; Burchart, 1968, 1970; Skupiński, 1975) and many others, brought some basic knowledge of their geologic structure, stratigraphy and metamorphic evolution. We have aimed our study to the problems of metamorphism in the south-western part of the Western Tatra Mts. crystalline complexes where metamorphic rocks are most frequently occuring from the Western and High Tatra Mts. and where progressive increase of metamorphism caused the formation of metamorphic zones (Figs. 1, 2).

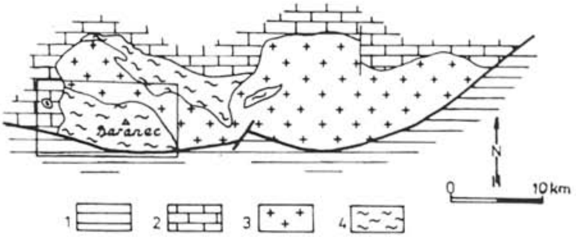

Fig. 1. Geologic sketch of map of High and Western Tatra Mts. with marked studied area.
Explanations: 1 — Paleogene; 2 — Mesozoic; 3 — granitoids; 4 — metamorphites.

Geologic setting

The Western Tatra Mts. crystalline complexes between the Jalovecká and Račková valleys (Fig. 2) are formed by pre-Mesozoic complexes of metamorphic and granitoid rocks. On the basis of their mutual position, the following profile

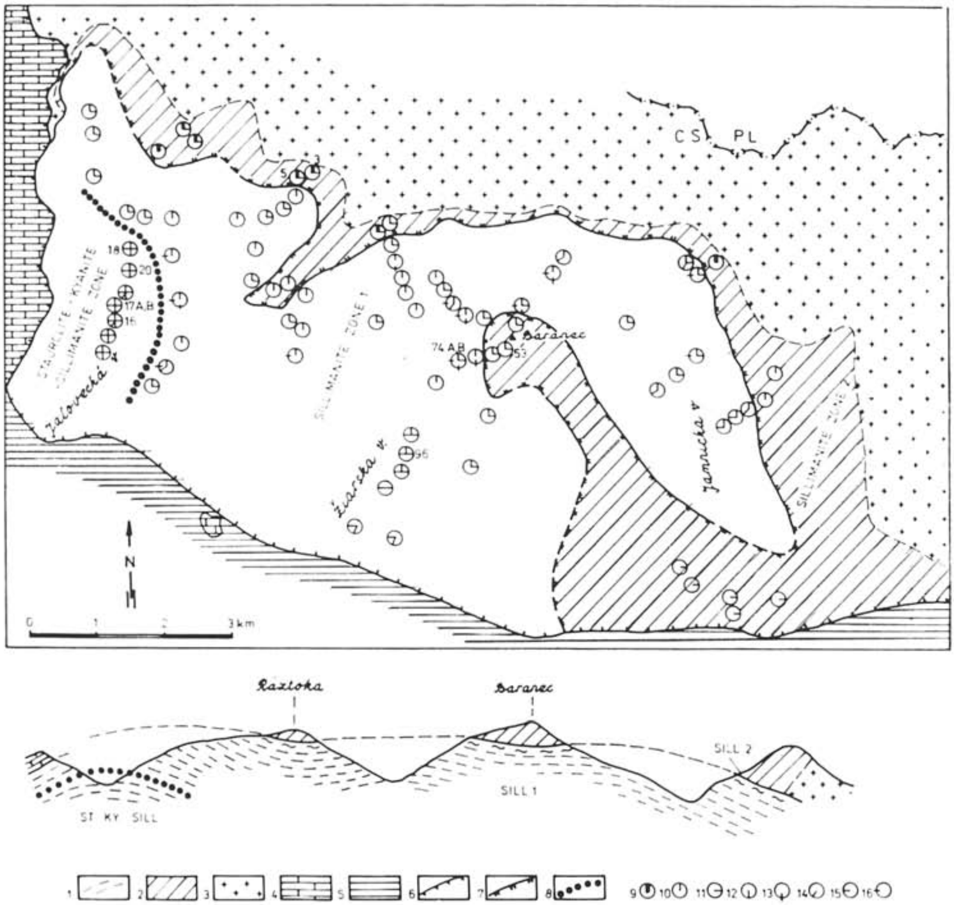

Fig. 2. Map of metamorphic zoning in SW part of Western Tatra Mts. crystalline complexes based on tectonic sketch of Kahan (1969).

Explanations: The course of the profile is from W to E across the elev. point Baranec. Localities and mineral assemblages of metapelites are marked by circles, numbered circles are samples analysed on microprobe.
1 — basement metamorphite complex A (see text); 2 — metamorphite complex B (see text); 3 — granitoids; 4 — Mesozoic; 5 — Paleogene; 6 — tectonic lines; 7 — thrust plane of granitoid and migmatite complex; 8 — metamorphic isograd; 9 — crystalline sillimanite; 10 — fibrolitic sillimanite; 11 — garnet; 12 — staurolite; 13 — staurolite relics; 14 — chloritoid; 15 — kyanite; 16 — kyanite relics.

can be distinguished, with an approximate thickness of 1000–1300 m (Kahan, 1969):

A – basement complex formed by schists, schistose gneisses, paragneisses, quartzite-gneisses, metaquartzites, orthogneisses (granite-gneisses), migmatites and amphibolites;

B – complex of paragneisses, amphibolites, migmatites and hybride granites in immediate contact with the above lying granitoids;
C – granitoids;
D – complex of paragneisses, quartzitic gneisses, migmatites and amphibolites above the granitoids.

The complex D does not occur on the studied territory, but more to east and it represents smaller bodies, especially in the area of Bystrá and Veľká Kamenistá.

On the basis of the study of tectonic elements, a dome-like structure was found in the region of Baranec and Ráztoka (Gorek, 1956, 1959; Kahan, 1969), faulted by partial block displacements and folding (Fig. 2). The course of foliation S_1 of metamorphic schistosity in the distinguished complexes is variable, differing from each other. The prevailing direction of b-axes of folds in the basement complex A is NE-SW, with a vergency to south as well as to north. The foliation S_2 is younger, it cross-cuts frequently the foliation S_1, or it causes bending of its planes. It is evidently connected with the formation of diaphtorites and phyllonites in which the planes S_2 are developed most prominently. As far as Hercynian as well Alpine diaphtorite zones (Gorek, 1967) are concerned, a very prominent one is the flat diaphtorite-phyllonite dislocation which can be observed in varying thickness along the contact of the basement complex A with the complex B (Fig. 2). It is probably the case of re-activation of an older fault zone where it was most exposed; the granitoid complex together with its migmatite mantle was thrusted along this zone on the basement metamorphic complex. This is probably a Hercynian-prepared plane of mechanical inhomogeneity; at the same time, it is necessary to consider the complicated Alpine tectonics of nappe character. A more detailed analysis of tectonic elements can be found in the work of Kahan (1969). The study of tectonic elements revealed the effects of at least two tectonic cycles – Hercynian and Alpine, while the existence of a cycle older than Hercynian has not been supported by sufficient evidence; this is in accordance with the geochronological data.

Geochronological data from the Western and High Tatra Mts. crystalline complexes indicate Hercynian age of the granitoids and of the majority of metamorphites. The data of Kantor (1959) obtained by K-Ar method gave the age 226–278 m.y. for mylonites. Burchart (1968) obtained by Rb-Sr method the age 290–300 m.y. for the main granitoid body of the High Tatra Mts., leucogranites (alaskites) and pegmatites of the Western Tatra Mts. and for quartz-diorites and alaskites from the region of Goryczkowa. The same age was determined for the recrystallization of metamorphites of the Western Tatra Mts. and Goryczkowa (Burchart, 1968, 1969). Metamorphic recrystallization appears to be simultaneous with the crystallization of granitoids intruding during the culmination of regional metamorphism or immediately afterwards. There is no satisfactory proof for the time of onset of metamorphic activity. The whole-rock isochrone from the Goryczkowa gneisses indicated the age 410–430 m.y. corresponding to the age of an older, probably Caledonian isotope homogenization. Datings by the Rb-Sr method (Burchart, 1968) also did not registrate any process corresponding to a younger – Alpine – recrystallization; thus, the effects of Alpine orogeny were above all cataclasis and mylonitization, with no higher-temperature metamorphic effects (Burchart, 1968). Data obtained by the Pb-U method (Cambel et al., 1977) indicated for a gneiss from the region of Račková Valley in Western Tatra Mts. the age 550 m.y. (the authors mention as much as 80 % of clastogene zircon) and for a migmatite the age 315 m.y.

Brief characterization of lithology of the metamorphites

Previous studies of metamorphic lithology in the Western Tatra Mts. crystalline complexes (Koutek, 1935; Gorek, 1959; Kahan, 1967) revealed the flyschoid character of the original sedimentation, belonging probably to the turbidite facies. Several cm, dm to m thick lamines, beds and layers of metapelites and metapsammites are here alternating.

Metapelites are represented by schists, schistose gneisses and paragneisses; their more detailed characteristics shall be presented in the following passage.

The metapsammites correspond to gneisses, quartzite-gneisses and metaquartzites with varying grain-size, from fine-grained metaquartzites and quartzite-gneisses to coarse grained gneisses. In their pre-metamorphic evolution they evidently corresponded to quartzose sandstones and graywackes. Metabasites form only small bodies concordant with the foliation of the metapelites and metapsammites and they have the form of interbedded intrusions and veins. Most frequently they occur in the complex B, especially as fine- and medium-grained amphibolites, coarse-grained gabbro-amphibolites and banded amphibolites. Metabasite bodies are found in the complex A, mainly in the lower parts of the Žiarska and Trnovecká valleys, where they correspond predominantly to fine- and medium-grained "paraamphibolites" impregnated by pyrite. The metabasites are characterized in a similar way by Gorek (1959). Except for some rare occurences, metabasites are practically totally missing in the monotonous profile of metapelites and metapsammites on the southern slopes of Baranec with an approximate thickness of 1000 m.

In the basement complex A, bodies of so-called "orthogneisses" and granite-gnesisses occur above all in the lower parts of the Žiarska and Trnovecká Valleys and on the southern slopes of Baranec. They form several dm to m thick bodies and veins, predominantly concordant with the strongly diaphtorized so-called "older" migmatites. The veins are sometimes as much as several tens of meters thick, they are relatively clearly separated from the surrounding rocks and they have intrusive character. A more detailed description was presented by Koutek (1935) and Gorek (1959). On the basis of their granitic composition, structure and texture, these rocks can be classified rather as granite-gneisses formed by crystallization of granite melt in syntectonic conditions.

Migmatites

In the area of granite-gneiss and amphibolite occurences in the basement complex A, strongly diaphtorized, so-called "older" migmatites are found; their origin is connected with regional metamorphism in syntectonic conditions. Diaphtoresis makes the determination of their primary character and of the conditions of their formation rather complicated; we aimed our attention therefore to migmatites occuring on contact with granitoids in the complex B –

the so-called "younger" migmatites (Gorek, 1959). The origin of the "younger" migmatites was connected with the effects of tongue-shaped granitoid body intruding into regionally metamorphosed rocks and causing the formation of injection and metasomatic migmatites (Gorek, 1959).

The studied migmatites, regardless of their origin, correspond to stromatitic as well as to more homogeneous types with large plagioclase crystals which can be classified rather as augen gneisses and only partly as ophtalmitic migmatites (e. g. Mehnert, 1968). The bands in the stromatitic migmatites are more differentiated, their thickness ranging from 2–3 mm to 10 mm and more. Paleosome (mesosome), leucosome and melanosome (Johannes, 1983) can be quite well distinguished and their composition was controlled evidently by the lithology of the pre-existing rocks. The paleosome of stromatites formed from Al-rich metapelites has a composition similar to the surrounding paragneisses. Except quartz, plagioclase, biotite and muscovite it contains considerable amounts of sillimanite and garnet. Leucosome is usually more coarse-grained and it consists mostly of quartz and plagioclase, sometimes with K-feldspar (microcline). Some of the migmatite types with predominant leucosome correspond to metatexites and diatexites which have leucosome of granite composition. Melanosome consisting of biotite is in some cases not clearly distinguishable or it is absent. From the study of P-T conditions (in the following section) it follows that migmatites were formed predominantly in the conditions of high-grade metamorphism as a result of metamorphic differentiation and partial anatexis.

Metamorphism and metamorphic zones

Data from geochronology and the study of structural-tectonic elements indicate that the metamorphic evolution of the Western Tatra Mts. crystalline complexes was most intensively affected by the Hercynian orogeny, corresponding to a cycle of progressive and retrograde metamorphic changes defined by the character and evolution of mineral assemblages in various metamorphic conditions. The Alpine orogeny did not metamorphically affect the earlier formed zoning of crystalline complexes, but it re-worked tectonically their geologic structures and disturbed the distribution of metamorphic zones in space. Tectonic effects of the Alpine as well as Hercynian orogenies caused also diaphtoresis, mylonization and cataclasis, the age determination of which is in many cases problematic. The object of our study was above all progressive metamorphism of the crystalline complexes and the related metamorphic zoning.

The progressive increase of metamorphism showed in the changes of mineral assemblages, above all in metapelites, thus allowing the determination of progressive metamorphic zones in the SW part of the Western Tatra Mts. crystalline complexes on the basis of field and microscopic studies.

Staurolite-kyanite-sillimanite zone: is characterized on the basis of the presence of staurolite, kyanite and fibrolitic sillimanite in metapelites, with additional garnet, biotite, muscovite, plagioclase, quartz and ilmenite as a mineral assemblage of progressive metamorphism. In rocks affected by retrograde metamorphism, chlorite, chloritoid, muscovite, margarite and tourmaline are formed as products of the breakdown of higher-temperature progressive-metamorphic assemblage. We can assume that, with the elimination of retrograde minerals, the progressive mineral assemblage was during peak metamorphic conditions approximately in equilibrium.

The coexistence of kyanite and sillimanite from the viewpoint of their stability can be analysed on the basis of several criteria:

a) According to the phase rule, two polymorphs of Al_2SiO_5 can coexist stabily only on the curve of univariant equilibrium separating their stability fields.

b) The presence of trace elements ("impurities"), e. g. Fe^{3+}, Mn^{3+} (Albee — Chodos, 1969; Grambling — Williams, 1985), as another degree of freedom, can stabilize the polymorphs in a divariant stability field, in a certain P-T interval, even after overstepping the curve of univariant equilibrium.

c) Direct-transformation reactions of Al_2SiO_5 polymorphs of the solid-solid type take place at small changes of entropy and they require considerable overstepping of equilibrium conditions; this results also in the slow rate of these reactions in near-equilibrium conditions.

From the calculations of temperature and pressure on the basis of thermobarometry (Tab. 6) it follows that the P-T conditions of kyanite-sillimanite coexistence are near to the conditions of univariant equilibrium curve of kyanite and sillimanite according to Holdaway (1971).

Trace elements studied by microprobe do not attain quantities which could more substantially influence the stability of Al_2SiO_5 polymorphs. In the kyanite coexisting with fibrolitic sillimanite, only low contents of Fe^{3+}, Mn^{3+} and Cr^{3+} have been determined (Tab. 2.)

Certain overstepping of equilibrium conditions is probable with the observed microstructure relations of kyanite and sillimanite, which usually coexist mutually separated; from kinetics it follows that their mutual reactions are controlled above all by diffusion (Fisher, 1978; Walther — Wood, 1984; Rubie — Thompson, 1985). Kyanite and sillimanite can therefore coexist metastably in a certain temperature and pressure interval even after overstepping of equilibrium conditions.

Sillimanite zone 1: represents the lower-temperature part (subzone) of the sillimanite zone. Sillimanite zone 1 is noted for the presence mostly of only fibrolitic sillimanite, by the disappearance of staurolite and partly also of kyanite. The breakdown of staurolite and kyanite is not simultaneous, but kyanite remains along with sillimanite or without it in the lower-temperature part of the sillimanite zone. An independent kyanite zone could not so far be distinguished in the studied region; its presence could be indicated by kyanite occurences in the lower part of the Žiarska Valley, on the southern slopes of Baranec and in the Jamnická Valley (Fig. 2). Garnet remains stabile or it breaks down, depending evidently also on the bulk composition, as garnet is usually stabile in rocks with higher iron contents.

Sillimanite zone 2: is characterized by the presence of prismatic sillimanite. Staurolite and kyanite are entirely absent, neither have they been determined in the form of relics which are present in the sillimanite zone 1. Garnet forms rather large porphyroblasts with no noticeable signs of retrogression. The amount of biotite, sillimanite and plagioclase is higher in comparison with lower-temperature zones, while the quantity of muscovite and quartz is decreased. The presence of K-feldspar, formed by breakdown of muscovite, has not been observed. K-feldspar (microcline) is present above all in the migmatite leucosome and it was formed probably already in the conditions of partial melting. We have therefore not distinguished an independent sillimanite-K-feldspar zone of high-grade metamorphism, known from many regions (e. g. Evans — Guidotti, 1966; Tracy, 1978).

The transition from the staurolite-kyanite-sillimanite zone into the sillimanite zone can be expressed by an isograd on the basis of the observed breakdown of staurolite with the formation of sillimanite. Isograd should be understood as a line on the present surface expressing specific changes in the observed mineral assemblages resulting from metamorphic reactions (Carmichael, 1970). In the studied region, the isograd between the staurolite-kyanite-sillimanite zone and the lower-temperature part of the sillimanite zone — sillimanite zone 1 — lies within the basement complex A in the area of Jalovecká Valley (Fig. 2). Partial breakdown of staurolite as well as of kyanite and garnet accompanied by the formation of sillimanite took place not only on the isograd, but also within the staurolite-kyanite-sillimanite zone; this is in accordance with the microscopic observations.

On the basis of petrographic criteria as well as for the purpose of expressing different P-T conditions of metamorphism, the sillimanite zone has been divided into two subzones. The lower-temperature part of the sillimanite zone is represented predominantly by schists and schistose gneisses, to a lower extent by gneisses. Gneisses and migmatites occur in the higher-temperature part of the sillimanite zone. The boundary between the sillimanite zone 1 and 2 is not defined by any isograd because there are no changes in mineral assemblages. An evidence of a progressive increase of temperature within the sillimanite zone is the breakdown of staurolite and kyanite which are entirely absent in the sillimanite zone 2, where solidus conditions were overstepped causing the formation of melt in migmatites.

The boundary between the sillimanite zones 1 and 2 in the map of metamorphic zoning (Fig. 2) is practically identical with the boundary between the complex of metamorphic rocks A and the complex B, which in many places has been proved to be of tectonic origin (Kahan, 1969). Along this thrusting plane, tectonic faulting and a reduction of the original width and course of the sillimanite zone took place; the lower-temperature part of the zone corresponds to the basement complex A and the higher-temperature part to the overthrusted complex B. The staurolite-kyanite-sillimanite zone occurs only in the basement complex A in the SW part of the region in Jalovecká Valley, where we assume its submergence under Mesozoic formations and the massif of Ráztoka and Baranec (Fig. 2). The isograd between the staurolite-kyanite--sillimanite zone and the sillimanite zone was probably folded simultaneously with the formation of fold structures in the crystalline complexes.

Metamorphic textures and minerals of metapelites

Chemical composition of the studied minerals was analysed with the help of the electrone microanalyser JEOL JXA-5A, using the method of Bence —

Albee (1968) and the correction factors of Albee – Ray (1970), on the Faculty of Chemical Technology of the Slovak Institute of Technology in Bratislava. Kyanite was analysed on the microanalyser JEOL SUPERPROBE 733 on the Dionýz Štúr Geological Institute in Bratislava. Chemical analyses of minerals are presented in Tabs. 1—5, with formulas calculated on the basis of oxygen anions. All iron is considered to be bivalent, except for kyanite, where it is considered to be trivalent. We have analysed representative samples from the staurolite-kyanite-sillimanite zone and from sillimanite zones 1 and 2 suitable for the calculation of P-T conditions of metamorphism*. Localization of the analyzed samples is in the map of metamorphic zoning in Fig. 2.

Garnet:

In the staurolite-kyanite-sillimanite zone it forms individual porphyroblasts or it is enclosed in staurolite (Fig. 3), kyanite or plagioclase. In the central part of grain it is often resorbed and it forms atoll texture.

The edge of garnet is sometimes crossed by intergrowths of sillimanite with biotite which grow inside the atoll texture (Fig. 4), or they form pseudomorphs after garnet from which only relics have been preserved (Fig. 5). From retrograde alterations of garnet, chloritization is the most frequent one; sporadically chloritoid is formed together with chlorite and fine-grained muscovite. In the sillimanite zone 1, the microstructure character of garnet is similar, but it does not coexist with staurolite. In the sillimanite zone 2 it forms large porphyroblasts (Fig. 10), sometimes it encloses biotite and only very rarely also prismatic sillimanite. Staurolite or kyanite inclusions have not been observed. Retrograde alterations of garnet in the sillimanite zone 2 are more rare than in garnets from lower-temperature zones; the grain-rims are sometimes resorbed.

Chemical composition of garnet (Tab. 1) corresponds predominantly to almandine, garnets of the sillimanite zones have increased contents of the

---

* Samples 16, 17A, 17B, 18 and 20: staurolite-kyanite-sillimanite-garnet two-mica schists to schistose gneisses, well-foliated and deformed, with veinlets of secretion quartz. Sample 16 contains retrograde chloritoid and margarite. Staurolite-kyanite-sillimanite zone. Jalovecká Valley, rock exposures on the right side of the creek Jalovčianka in the central part of the valley.

Samples 74A, 74B: garnet-sillimanite-muscovite-biotite gneisses with sporadic relics of staurolite and kyanite. Sillimanite zone 1. Southwestern glen from the peak of Baranec (2184 m), leading into the Žiarska Valey, 1650 m above sea level.

Sample 96: garnet-kyanite-sillimanite-muscovite-biotite gneiss. Sillimanite zone 1. Lower part of the Žiarska Valey, rock exposure near the road to the Žiarska chalet, 1020 m above sea level.

Samples 3, 5: garnet-sillimanite-muscovite-biotite-plagioclase gneisses to migmatites. Noticeable banding is defined by layers with a thickness of 1—2 mm, rich in biotite, sillimanite, muscovite and garnet, alternating with more coarse-grained granular quartz-plagioclase layers up to 1 cm thick. Sillimanite zone 2. Upper part of the Valley Parichvost, rock exposures above the source of the creek Jalovčianka, towards Banikovské Saddleback.

Sample 53: muscovite-biotite-plagioclase "augen" gneiss, with a smal amount of garnet and sillimanite. Coarse-grained rock with large crystals of plagioclase with a size of 0.5—1 cm, relatively homogeneous. Sillimanite zone 2. Western ridge from the peak of Baranec (2184 m) leading into the Žiarska Valley, 2050 m above sea level.

Table 1

Chemical analyses of garnet

Zone	staurolite-kyanite-sillimanite								sillimanite 1				sillimanite 2				
sample	17A		17B		18		20		74A	74B		96	3		5	53	
analysis No	13c	15r	38c	42r	21c	20r	4c	5r	3r	9c	8r	7r	11c	1r	19r	8c	5r
SiO_2	37.29	37.04	37.17	37.09	36.70	37.05	36.21	36.60	36.91	36.98	37.36	37.51	36.81	37.04	37.29	37.02	36.70
TiO_2	0.00	0.04	0.03	0.02	0.00	0.00	0.18	0.06	0.00	0.00	0.00	0.00	0.01	0.02	0.00	0.04	0.03
Al_2O_3	21.32	21.27	20.81	21.84	20.92	21.17	21.47	21.42	21.16	21.47	21.32	21.04	21.46	21.13	20.51	20.88	21.03
FeO	34.86	34.56	34.63	34.43	35.76	36.11	37.14	36.37	34.20	32.51	32.37	31.12	29.88	30.09	30.42	35.67	33.02
MnO	2.84	2.98	3.17	3.03	3.25	2.86	2.49	2.29	4.89	6.17	6.29	6.61	8.97	9.06	9.07	3.09	6.31
MgO	2.53	2.63	2.15	2.42	1.87	2.26	1.52	2.15	2.91	3.38	2.73	3.48	2.42	2.30	2.55	3.37	2.27
CaO	1.88	1.63	1.96	1.91	2.01	2.00	1.16	1.30	0.90	0.36	0.92	1.27	1.40	1.37	1.01	1.14	1.30
Total	100.77	100.15	99.92	100.74	100.51	101.45	100.17	100.19	100.97	101.37	100.99	101.03	100.95	101.01	100.86	101.21	100.66
	Cations per 12 oxygens																
Si	2.983	2.988	3.013	2.972	2.978	2.972	2.959	2.969	2.986	2.958	2.992	2.995	2.962	2.981	3.006	2.970	2.971
Ti	0.000	0.002	0.002	0.001	0.000	0.000	0.010	0.004	0.000	0.000	0.000	0.000	0.000	0.000	0.000	0.002	0.002
Al	2.007	2.020	1.984	2.059	1.997	1.998	2.063	2.045	2.014	2.021	2.012	1.977	2.032	2.001	1.949	1.971	2.003
Fe	2.328	2.378	2.344	2.304	2.423	2.419	2.532	2.464	2.310	2.172	2.168	2.074	2.007	2.022	2.052	2.389	2.232
Mn	0.192	0.203	0.216	0.206	0.223	0.194	0.171	0.156	0.334	0.417	0.427	0.446	0.603	0.616	0.619	0.209	0.431
Mg	0.307	0.316	0.259	0.289	0.226	0.269	0.184	0.259	0.350	0.402	0.326	0.413	0.289	0.275	0.306	0.402	0.273
Ca	0.181	0.140	0.170	0.163	0.174	0.171	0.102	0.112	0.105	0.073	0.079	0.108	0.120	0.117	0.087	0.097	0.112
Fe/Fe+Mg	0.833	0.880	0.900	0.888	0.914	0.900	0.932	0.902	0.868	0.843	0.869	0.834	0.874	0.880	0.870	0.856	0.890
X_{Al}	0.774	0.779	0.788	0.778	0.796	0.793	0.848	0.824	0.752	0.709	0.723	0.682	0.664	0.667	0.670	0.771	0.732
X_{Sp}	0.064	0.068	0.072	0.069	0.073	0.063	0.058	0.052	0.109	0.136	0.142	0.147	0.201	0.203	0.202	0.068	0.141
X_{Py}	0.102	0.106	0.087	0.098	0.074	0.088	0.062	0.087	0.114	0.131	0.109	0.136	0.095	0.091	0.100	0.130	0.090
X_{Gr}	0.060	0.047	0.057	0.055	0.057	0.056	0.032	0.037	0.025	0.024	0.026	0.035	0.040	0.039	0.028	0.031	0.037

$X_i = i/Fe + Mn + Mg + Ca$, Al — Almandine, Sp — Spessartine, Py — Pyrope, Gr — Grossular, c — core, r — rim.

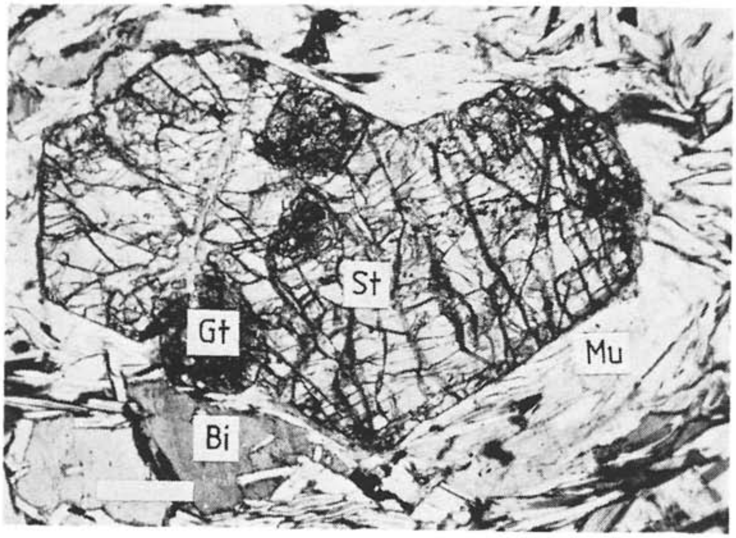

Fig. 3. Staurolite (St) enclosing garnets (Gt), surrounded by porphyroblasts of muscovite (Mu) and biotite (Bi).
Explanations: Schist, staurolite-kyanite-sillimanite zone, Jalovecká Valley. Parallel nicols, scale bar length 0.5 mm.

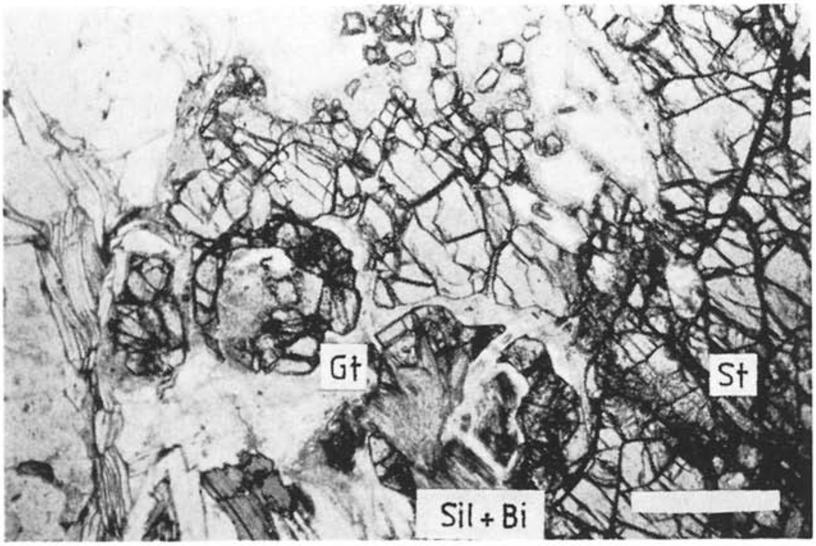

Fig. 4. Atoll garnet (Gt) cross-cut by intergrowths of fibrolitic sillimanite and biotite (Sil + Bi) growing inside the atoll texture of garnet. Staurolite (St) is present in the assemblage.
Explanations: Schist, staurolite-kyanite-sillimanite zone, Jalovecká Valley. Parallel nicols, scale bar length 0.5 mm.

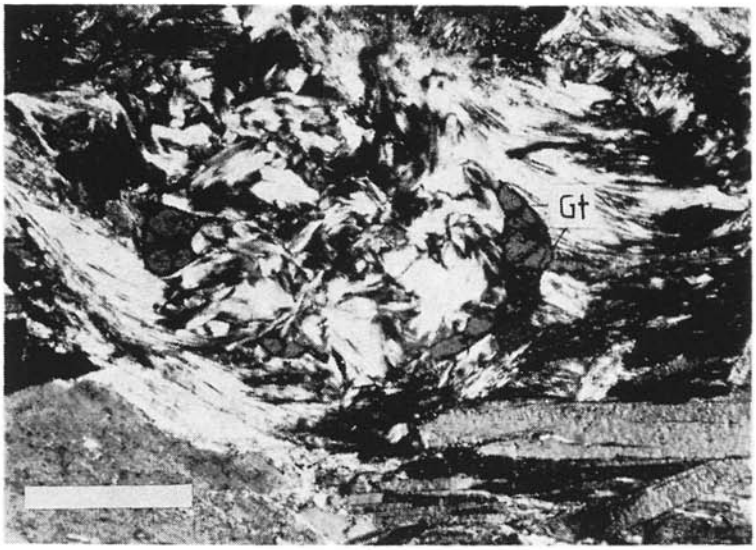

Fig. 5. Intergrowths of fibrolitic sillimanite and biotite replacing garnet from which only relics have been preserved.
Explanations: Schist, staurolite-kyanite-sillimanite zone, Jalovecká Valley. Crossed nicols, scale bar length 0.5 mm.

spessartite component. Distribution of elements on traverses across selected grains (Fig. 6) indicates zoning caused by the processes of growth and diffusion in different thermodynamic and kinetic conditions. Garnet from the staurolite-kyanite-sillimanite zone (sample 20) is almost homogeneous. The trend of element distribution is not pronounced, with a slight increase of Mg from core towards rim; it nevertheless decreases in immediate proximity of edge. The contents of Mn are relatively constant from core towards rim and they decrease near the edge. Fe decreases inconsiderably from core to rim and increases near edge. The contents of Ca are practically constant along all of the traverse. A grain from the sillimanite zone 2 (sample 3) has more pronounced zoning, with Mg and Fe increasing from centre towards the rim and then decreasing considerably near the edge. Mn has a reverse trend and Ca an approximately even course along the whole profile. The grain from the sample 53, also from the sillimanite zone 2, is noted for a decrease of Mg and Fe and an increase of Mn from core to the rim, while the contents of Ca do not change considerably. This zoning is characteristic for garnets from the high-temperature part of the sillimanite zone where a more rapid intracrystalline diffusion takes place at temperature approximately over 650 °C (Tracy, 1982).

Zoning of the studied garnets was controlled by nucleation and grain-growth rate as well as by diffusion rate in prograde as well as in retrograde P-T conditions of metamorphism. The original prograde growth zoning was modified to a varying extent by diffusion; we can assume that intracrystalline diffusion had effects at higher temperatures, especially in sillimanite zone 2, and intergranular diffusion took place during cooling and retrogression. Prograde zoning was characterized by an increase of Mg and decrease of Mn as well as by a decrease of the ratio Fe/Fe + Mg. The decrease of Mg, increase of Mn and increase of the ratio Fe/Fe + Mg in the rim of garnet were probably connected with continuous reactions of garnet with coexisting Fe-Mg-Mn minerals, especially with biotite, chlorite and ilmenite during cooling and retrogression, when re-equilibration of mineral composition occurred in lower P-T conditions.

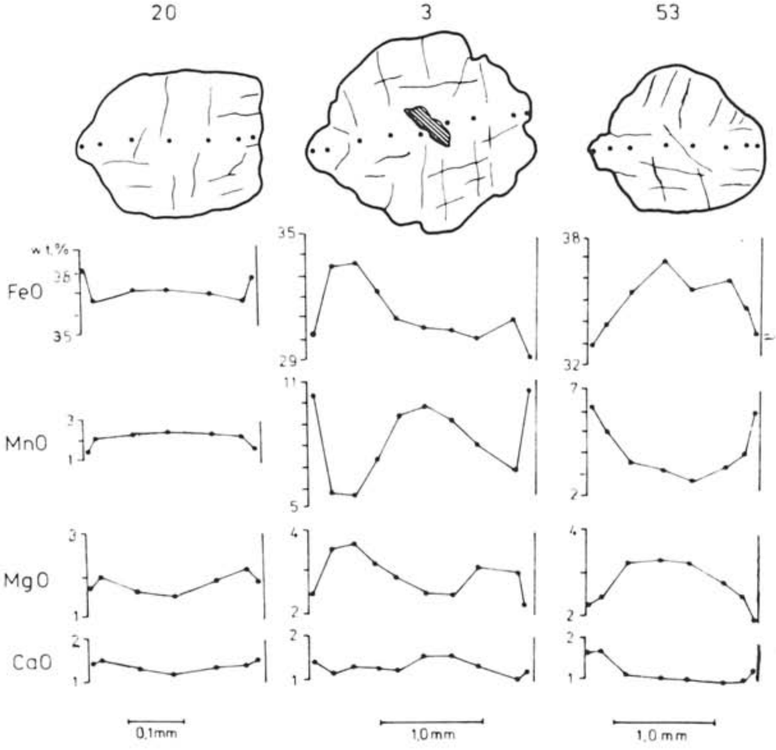

Fig. 6. Microprobe traverses across selected garnet grains.
Explanations: Sample 20 is garnet from the staurolite-kyanite-sillimanite zone, samples 3 and 53 are garnets from the sillimanite zone 2.

Staurolite:

forms porphyroblasts having typical sieve texture with poikilitic quartz, sometimes it also encloses garnet (Fig. 3). It is usually surrounded by muscovite, which can be of prograde or retrograde origin, and by biotite. It is quite difficult to identify prograde breakdown of staurolite due to its frequent retrogression. Muscovite rims, forming large flakes in contrast to the fine-flaked retrograde shimmer aggregate, could be the product of progressive breakdown of staurolite, as mentioned by Guidotti (1970) and Foster (1977) from the lower sillimanite zone in Maine, U.S.A.. In the sillimanite zone 1, staurolite relics are surrounded by muscovite porphyroblasts or they are isolated in plagioclase. Staurolite breakdown with direct formation of sillimanite has not been observed. Progressive breakdown of staurolite could therefore take place with the participation of muscovite, biotite, plagioclase and quartz. Staurolite retrogression resulted in the formation of fine-flaked muscovite, chlorite and sometimes small-prismatic chloritoid, which forms rims or preudomorphs around staurolite relics. Chemical composition of staurolite is in Tab. 2.

Kyanite:

Macroscopically visible kyanite crystals sometimes attain a size of several cm. They form segregations with muscovite and they occur mostly in veins of secretion quartz. Except the known occurences in the Jamnická and Račková Valleys (Kahan – Hvoždara, 1967), large kyanite crystals are found also in the lower part of the Žiarska Valley and on southern slopes of Baranec, near granite-gneiss bodies. Crystals with smaller size, visible mostly only microscopically, form a part of the mineral assemblage of the staurolite-kyanite-sillimanite zone and sometimes also of the sillimanite zone 1. Kyanite is usually surrounded by muscovite, biotite and quartz, sometimes it is enclosing garnet. Kyanite and sillimanite (fibrolite) are coexisting mostly mutually separated, without direct nucleation of sillimanite on kyanite, while sillimanite is formed from biotite or muscovite surrounding the kyanite (Fig. 7). Progressive breakdown of kyanite without direct transformation into sillimanite evidently took place by the way of local reactions, with a participation of muscovite, biotite and quartz. Direct transformation of kyanite into sillimanite is sporadic (Fig. 8). Thin-prismatic sillimanite crystals grow approximately parallelly with the cleavage of kyanite, in the direction of c-axis. As a result of retrograde processes, kyanite breaks down, and subsequently, white micas — muscovite and margarite — are formed; along with them, chloritoid is formed in microfissures of kyanite (Fig. 8). Chemical composition of kyanite coexisting with fibrolitic sillimanite without direct transformation is in Tab. 2. Kyanite contains very small amounts of Ti, Fe^{3+}, Mn^{3+}, Cr^{3+} and Mg.

Sillimanite:

is present in the form of fibrolite and prismatic crystals, while prismatic sillimanite is the diagnostic mineral of the sillimanite zone 2. Microstructural relations of sillimanite with other coexisting minerals are to a great extent variable. Fibrolite as well as prismatic sillimanite usually occur intergrown with biotite as well as with muscovite and sometimes they form isolated crystals or tiny needles in plagioclase and quartz. Fibrolite, together with biotite, muscovite and ilmenite, usually forms segregations, while the fibrolite often grows into the surrounding matrix and cross-cuts plagioclase and quartz grains. In some cases, fibrolite intergrown with biotite grows into the atoll garnet (Fig. 4), or it surrounds garnet relics (Fig. 5). The relation of sillimanite to kyanite has already been mentioned; kyanite and sillimanite (fibrolite) mostly coexist separately in different microscopic domains within one thin section, direct transformation of kyanite to sillimanite is rare (Fig. 8). Sillimanite is most frequently intergrown with biotite. Sillimanite crystals are oriented

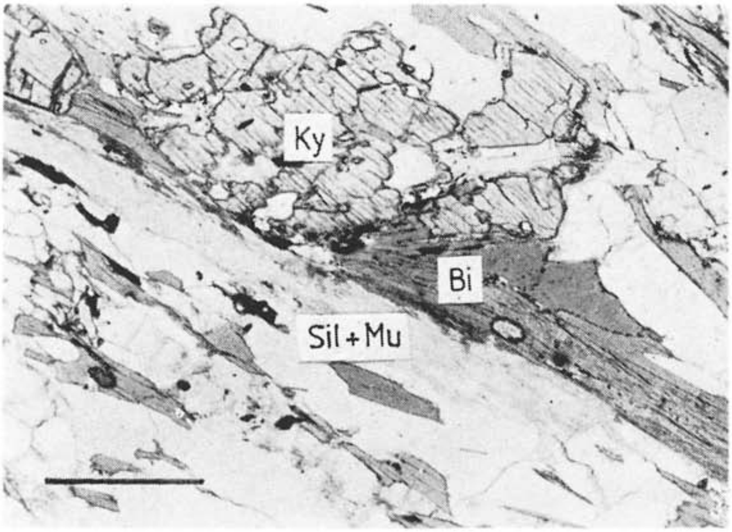

Fig. 7. Coexistence of kyanite (Ky) and Sillimanite (Sil) without direct transformation kyanite-sillimanite. Kyanite is surrounded by porphyroblasts of biotite (Bi) and muscovite intergrown with fibrolitic sillimanite (Sil + Mu).
Explanations: Gneiss, sillimanite zone 1, Žiarska Valley. Parallel nicols, scale bar length 0.5 mm.

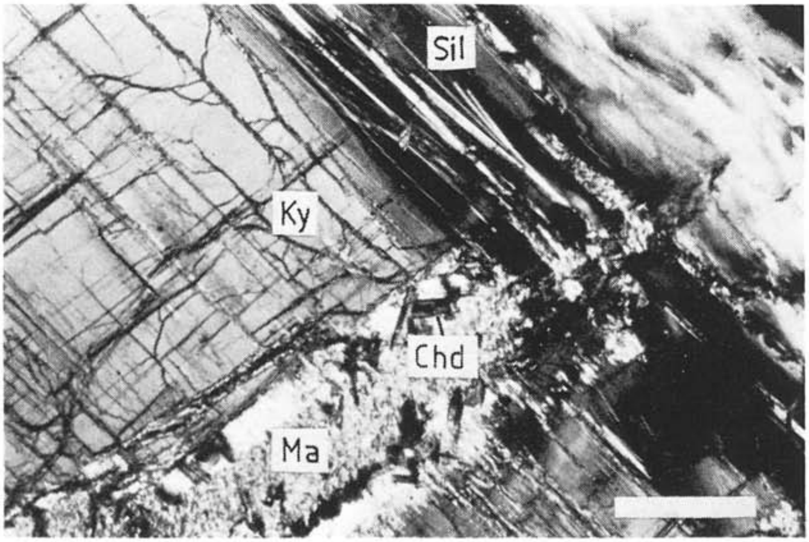

Fig. 8. Direct transformation of kyanite (Ky) into sillimanite (Sil). Thin-prismatic sillimanite crystals grown approximately parallelly with kyanite cleavage in the direction of elongation. Microfissure of kyanite is filled by minute margarite flakes (Ma) and small chloritoid prisms (Chd) formed in retrograde processes.
Explanations: Gneiss, sillimanite zone 1, Jamnická Valley. Crossed nicols, scale bar length 0.5 mm.

Table 2

Chemical analyses of staurolite, chloritoid and kyanite

	staurolite					chloritoid		
sample analysis No.	17A 3c	17A 5r	20 29c	20 34r	16 13c	16 12r	16 21	16 22
SiO_2	27.56	27.21	26.94	27.66	27.76	27.02	23.51	24.14
TiO_2	0.54	0.62	0.79	0.67	0.82	0.80	0.00	0.00
Al_2O_3	53.51	54.40	54.22	54.35	54.49	54.39	40.64	41.05
FeO	13.48	12.61	14.76	14.58	12.97	13.70	26.04	25.76
MnO	0.23	0.21	0.18	0.14	0.18	0.18	0.47	0.68
MgO	1.03	1.21	1.00	0.84	0.95	0.93	2.22	2.08
Total	96.35	96.26	97.89	98.24	97.17	97.02	92.90	93.71
	Cations per 46 oxygens						12 oxygens	
Si	7.743	7.637	7.522	7.673	7.723	7.657	1.956	1.985
Ti	0.112	0.129	0.161	0.138	0.169	0.162	0.000	0.000
Al	17.760	17.963	17.817	17.746	17.844	17.923	3.980	3.972
Fe	3.162	2.955	3.441	3.377	3.013	3.204	1.809	1.769
Mn	0.053	0.048	0.041	0.032	0.041	0.042	0.032	0.046
Mg	0.429	0.505	0.415	0.346	0.392	0.386	0.274	0.254
Fe/Fe+Mg	0.880	0.854	0.892	0.907	0.884	0.892	0.868	0.874

	kyanite	
	96 1	96 4
SiO_2	37.16	36.86
TiO_2	0.00	0.02
Al_2O_3	62.88	61.89
Fe_2O_3	0.21	0.21
Mn_2O_3	0.14	0.00
Cr_2O_3	0.00	0.07
MgO	0.00	0.02
Total	100.39	99.07
	5 oxygens	
Si	1.000	1.005
Ti	0.000	0.009
Al	1.992	1.986
Fe^{3+}	0.004	0.004
Mn^{3+}	0.002	0.000
Cr^{3+}	0.000	0.001
Mg	0.000	0.000

c — core, r — rim.

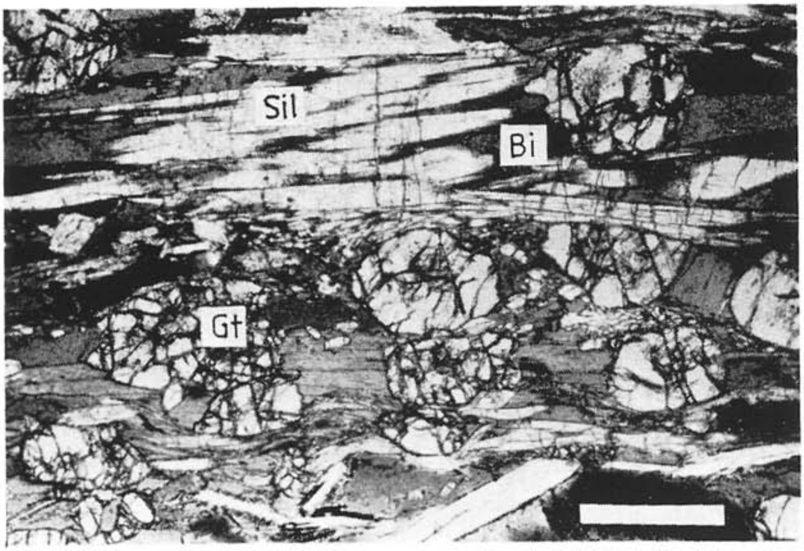

Fig. 9. Prismatic sillimanite (Sil) oriented subparallelly with the cleavage of biotite (Bi) with which it is intergrown. The assemblage contains garnet (Gt) with grains slightly deformed in the direction of foliation.
Explanations: Gneiss, sillimanite zone 2, Valley Parichvost. Parallel nicols, scale bar length 0.5 mm.

parallelly with the cleavage of biotite (Fig. 9), or under various angles, while sillimanite frequently grows from biotite into the surrounding minerals. The interpretation of relation sillimanite-biotite is not unambiguous. Sillimanite did not only grow preferentially from pre-existing biotite (epitaxial model of Chinner, 1961), but it was evidently also formed simultaneously with biotite, as a result of local reactions at the breakdown of staurolite, garnet and kyanite (Carmichael, 1969). A very frequent occurence is the growth of porphyroblasts of the so-called "late" muscovite around sillimanite and biotite; the orientation of this muscovite is different from the parallel orientation of biotite and sillimanite crystals (Fig. 10).

In many cases sillimanite is formed together with muscovite porphyroblasts from decomposing biotite, at the same time, ilmenite can be formed as well. Sillimanite, especially fibrolite, is often intergrown only with muscovite, or only with muscovite and quartz, with no signs of pre-existing biotite.

Symplektites of biotite with sillimanite in retrograde processes breakdown, consequently forming chlorite, muscovite, ilmenite and sometimes chloritoid.

Biotite:

It forms subhedral crystals mostly elongated in the direction of foliation. It is often intergrown with sillimanite and muscovite, to a various extent it is affected by chloritization. The observed change of pleochroism from light--brown(brown to dark-brown)reddish-brown evidently depends on the increase

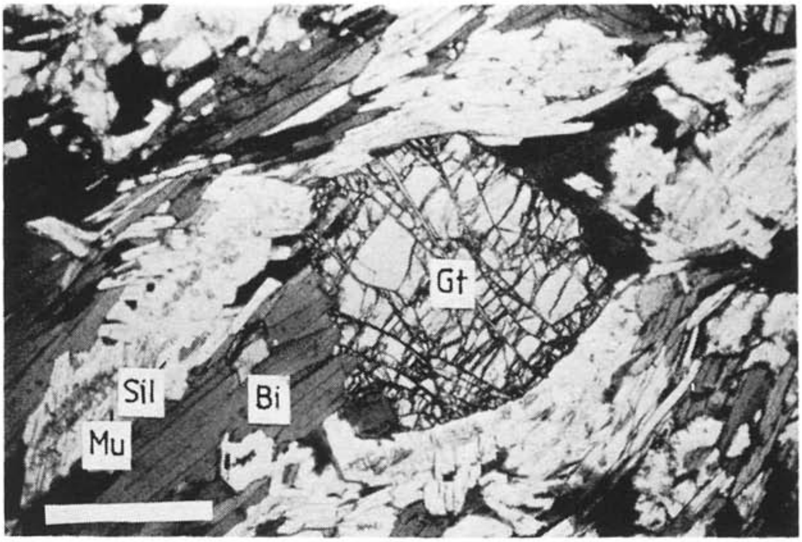

Fig. 10. Porphyroblast of garnet (Gt) surrounded by flakes of biotite and "late" muscovite (Mu) enclosing sillimanite needles (Sil). The orientation of muscovite is transversal to the subparallel orientation of biotite and sillimanite.
Explanations: Gneiss, sillimanite zone 2, Valley Parichvost. Parellel nicols, scale bar length 1.0 mm.

of metamorphism. The change of pleochroism is connected with the change of chemical composition of biotite showing in increased Ti and Fe contents in the highest-temperature sillimanite zone 2, as mentioned e. g. by Guidotti (1970). The composition of biotite is also affected by the bulk rock composition, from which follows also the increased Mn content in biotites from the sillimanite zone 2. Chemical composition of biotite is in Tab. 3.

Muscovite, margarite:

Muscovite occurs either as large flakes, or it forms fine-grained shimmer aggregates. Large muscovite porphyroblasts are oriented parallelly in foliation planes or they grow transversally. They often surround grains of staurolite, kyanite and sillimanite, and they are in various angles intergrown with biotite (Fig. 8). From the viewpoint of crystallization succession, cross muscovite appears to be the last mineral — i. e. the so-called "late" muscovite, usually connected with processes of metasomatism as well as progressive metamorphism. Fine-grained muscovite is usually formed along the edges and in microfissures of decomposing staurolite, garnet and kyanite, and it often forms pseudomorphs after them together with other retrograde minerals.

Margarite has been identified in microfissures of kyanite along with muscovite, chloritoid and chlorite (Fig. 8). It forms minute flakes with low birefrigence; it has been identified by microprobe. It is probably formed after the breakdown of kyanite; the necessary Ca was evidently released from the

Table 3

Chemical analyses of biotite

zone	staurolite-kyanite-sillimanite				sillimanite 1			sillimanite 2			
sample analysis No.	17A 16	17B 41	18 23	20 1	74A 1	74B 14	96 3	3 10in	3 2	5 21	53 1
SiO_2	35.36	36.01	35.28	34.58	34.20	34.56	35.32	34.66	33.71	34.77	34.89
TiO_2	1.16	1.25	1.59	1.70	2.10	2.21	2.17	1.78	2.35	2.15	2.19
Al_2O_3	18.40	20.04	18.80	19.92	19.63	19.05	18.13	18.33	18.31	18.57	17.88
FeO	21.10	19.61	21.98	22.07	23.12	21.48	19.46	22.93	23.67	22.81	23.49
MnO	0.09	0.13	0.11	0.06	0.00	0.01	0.24	0.49	0.50	0.31	0.18
MgO	9.78	9.51	8.39	7.48	9.27	9.07	10.56	7.70	7.83	8.41	7.05
CaO	0.02	0.00	0.02	0.03	0.00	0.00	0.01	0.03	0.04	0.00	0.00
Na_2O	0.00	0.29	0.07	0.14	0.04	0.03	0.13	0.00	0.02	0.10	0.08
K_2O	9.20	9.12	9.14	9.21	8.59	9.08	9.33	9.27	9.23	8.87	9.31
Total	95.11	95.96	95.38	95.19	96.95	95.49	95.35	95.19	95.66	95.99	95.07
					Cations per 22 oxygens						
Si	5.434	5.422	5.467	5.337	5.195	5.305	5.39	5.395	5.253	5.346	5.449
Al^{IV}	2.566	2.576	2.533	2.663	2.805	2.695	2.61	2.605	2.742	2.654	2.551
Al^{VI}	0.766	0.979	0.847	0.955	0.704	0.745	0.646	0.753	0.619	0.706	0.735
Ti	0.134	0.142	0.182	0.196	0.227	0.243	0.248	0.207	0.274	0.247	0.255
Fe	2.712	2.469	2.804	2.845	2.933	2.753	2.480	2.980	3.083	2.929	3.063
Mn	0.012	0.016	0.013	0.007	0.000	0.000	0.030	0.064	0.065	0.039	0.023
Mg	2.240	2.134	1.908	1.719	2.096	2.072	2.399	1.784	1.817	1.924	1.639
Ca	0.002	0.000	0.182	0.004	0.000	0.000	0.000	0.004	0.006	0.000	0.000
Na	0.000	0.085	0.002	0.041	0.010	0.008	0.036	0.000	0.005	0.029	0.023
K	1.804	1.752	1.778	1.810	1.661	1.774	1.812	1.838	1.833	1.787	1.851
Fe/Fe+Mg	0.547	0.536	0.595	0.623	0.583	0.571	0.508	0.625	0.629	0.603	0.651
X_{Ann}	0.462	0.428	0.487	0.497	0.492	0.473	0.427	0.514	0.526	0.501	0.536
X_{Ph}	0.382	0.370	0.331	0.300	0.351	0.356	0.413	0.308	0.310	0.329	0.287

$X_i = i/Fe + Mg + Mn + Al^{VI} + Ti$, Ann — Annite, Ph — Phlogopite, in — inclusion in garnet core.

anorthite component of plagioclase due to the effects of fluids during retrograde metamorphism.

Chemical composition of muscovite and margarite is presented in Tab. 4. Muscovite is approaching the ideal composition, with a very low content of the celadonite component, which is higher only in fine-grained muscovite. The amount of the paragonite component slightly decreases with increasing grade of metamorphism and Ti-content increases. The ratio of iron to magnesium changes similarly as in the coexisting biotite. The relations of muscovite chemistry to metamorphic grade are similar as those mentioned by e. g. Guidotti (1984).

Chloritoid:

It forms small prismatic crystals with typical lamelling, often in fan-like aggregates. It is formed by retrograde reactions, especially from staurolite, garnet, kyanite, biotite and sillimanite (Fig. 8). Chemical composition of chloritoid is in Tab. 2.

Plagioclase:

The composition of plagioclase analysed by microprobe (Tab. 5) corresponds to oligoclase (An_{14-32}). It is mostly homogeneous, a more prominent zoning has not been observed. Plagioclases in augen gneisses and migmatites attain a size of 1—2 cm and more. Megacrystals are partially deformed and they have pre-tectonic character of growth compared with the minerals of the matrix which flow around them. Chemical composition of large crystals is homogeneous and same as that of small grains.

Metamorphic reactions

The transition from the staurolite-kyanite-sillimanite zone to the sillimanite zone expressed by an isograd corresponds to staurolite breakdown and the formation of sillimanite. It can be expressed by the discontinuous reaction:

$$\text{staurolite} + \text{muscovite} + \text{quartz} = \text{biotite} + \text{sillimanite} + \text{garnet} + H_2O \quad (1)$$

The reaction (1) is univariant in the simplified metapelitic system K_2O-MgO-FeO-Al_2O_3-SiO_2-H_2O (KMFASH) — Thompson (1976a, b).

The reaction (1) is a result of separate continuous staurolite-breakdown reactions:

$$\text{staurolite} + \text{muscovite} + \text{quartz} = \text{biotite} + \text{sillimanite} + H_2O \quad (2)$$

$$\text{staurolite} + \text{quartz} = \text{garnet} + \text{sillimanite} + H_2O \quad (3)$$

or

$$\text{staurolite} + \text{Mg-biotite} + \text{muscovite} + \text{quartz} = \text{Fe-biotite} + \text{sillimanite} + H_2O \quad (2')$$

Table 4

Chemical analyses of muscovite and margarite

	muscovite								margarite	
zone	staurolite-kyanite-sillimanite					sillimanite 1	sillimanite 2		staurolite-kyanite--sillimanite	
sample	16	16	17	20	20	96	3	5	16	16
analysis No.	7s	23	17	37s	38	9	32	27	15s	30s
SiO_2	46.40	45.96	44.97	46.29	46.39	44.85	44.78	45.50	30.12	30.28
TiO_2	0.11	0.45	0.60	0.20	0.55	0.88	1.18	0.99	0.04	0.01
Al_2O_3	37.32	36.36	34.52	31.62	34.30	34.38	34.65	33.57	50.06	50.66
FeO	0.78	0.83	1.08	3.11	0.68	1.50	2.25	3.34	0.31	0.35
MnO	0.00	0.00	0.01	0.03	0.04	0.02	0.00	0.00	0.00	0.00
MgO	0.31	0.56	0.61	0.63	0.48	0.89	0.60	0.48	0.09	0.22
CaO	0.37	0.00	0.00	0.00	0.00	0.02	0.01	0.00	11.88	12.03
Na_2O	0.62	0.95	1.06	1.09	1.63	1.18	0.33	0.71	1.50	1.24
K_2O	9.24	9.38	10.56	9.97	9.66	9.24	10.72	10.39	0.01	0.00
Total	95.15	94.49	93.38	92.94	93.73	92.96	94.52	94.98	94.01	94.79
	Cations per 22 oxygens									
Si	6.173	6.120	6.145	6.363	6.254	6.095	6.065	6.153	4.060	4.044
Al^{IV}	1.827	1.880	1.855	1.637	1.746	1.905	1.935	1.847	3.940	3.956
Al^{VI}	4.018	3.818	3.696	3.486	3.703	3.609	3.588	3.504	4.002	4.008
Ti	0.010	0.044	0.061	0.031	0.056	0.089	0.119	0.101	0.002	0.000
Fe	0.086	0.091	0.122	0.357	0.077	0.170	0.254	0.377	0.034	0.038
Mn	0.000	0.000	0.000	0.003	0.005	0.001	0.000	0.000	0.000	0.000
Mg	0.060	0.110	0.123	0.129	0.096	0.179	0.120	0.098	0.017	0.043
Ca	0.052	0.000	0.000	0.000	0.000	0.002	0.000	0.000	1.715	1.721
Na	0.159	0.244	0.287	0.282	0.425	0.310	0.081	0.186	0.390	0.320
K	1.565	1.590	1.734	1.851	1.661	1.603	1.849	1.797	0.000	0.000
Fe/Fe + Mg	0.589	0.452	0.498	0.734	0.445	0.487	0.679	0.793	0.666	0.469
Na/Na + K	0.093	0.133	0.143	0.133	0.204	0.161	0.044	0.094	0.000	0.000

s — shimmer aggregate

Table 5

Chemical analyses of plagioclase

zone	staurolite-kyanite-sillimanite				sillimanite 1			sillimanite 2		
sample analysis No.	17A 21	17B 34	18 19	20 21	74A 5	74B 6	96 10	3 4	5 15	53 15
SiO_2	60.33	60.10	59.05	64.85	64.62	64.94	64.61	60.02	61.54	61.57
Al_2O_3	24.76	25.86	26.10	21.67	22.01	21.36	21.76	25.72	24.42	23.33
CaO	6.28	6.80	6.06	3.09	3.11	3.11	3.11	6.22	5.09	5.36
Na_2O	8.15	7.76	8.77	10.21	9.96	10.19	9.92	7.75	9.41	9.25
K_2O	0.07	0.06	0.11	0.07	0.10	0.09	0.10	0.13	0.08	0.05
Total	99.59	100.58	100.09	99.89	99.80	99.69	99.50	99.84	100.54	99.56
Cations per 8 oxygens										
Si	2.692	2.661	2.635	2.860	2.854	2.873	2.859	2.672	2.722	2.750
Al	1.299	1.367	1.373	1.126	1.144	1.112	1.134	1.348	1.273	1.228
Ca	0.300	0.322	0.290	0.146	0.147	0.147	0.147	0.296	0.241	0.257
Na	0.704	0.665	0.759	0.873	0.851	0.872	0.850	0.668	0.807	0.801
K	0.003	0.003	0.006	0.004	0.005	0.005	0.005	0.007	0.005	0.003
X_{Ab}	0.699	0.672	0.719	0.853	0.848	0.851	0.848	0.693	0.766	0.755
X_{An}	0.298	0.325	0.275	0.143	0.147	0.144	0.146	0.300	0.229	0.242
X_{Or}	0.003	0.003	0.006	0.004	0.005	0.005	0.006	0.007	0.006	0.003

$X_i = i/Na + Ca + K$, Ab — Albite, An — Anorthite, Or — Orthoclase

$$\text{staurolite} + \text{Fe-garnet} + \text{quartz} = \text{Mg-garnet} + \text{sillimanite} + H_2O \qquad (3')$$

The observed breakdown of garnet with the formation of sillimanite and biotite in the staurolite-kyanite-sillimanite zone and in the sillimanite zone 1 could take place according to the reaction:

$$\text{garnet} + \text{muscovite} = \text{biotite} + \text{sillimanite} + \text{quartz} \qquad (4)$$

expressing in the system KMFASH the disappearance of "pure" Fe-Mg garnet after the breakdown of staurolite. The observed breakdown of garnet in the presence of staurolite could be caused by an admixture of Ca and Mn in garnet.

Continuous reactions in the system KMFASH lead to a change in the ratio of iron to magnesium in the reaction products with increased temperature (Thompson, 1976a, b). The reactions (2), (2') and (4) lead to an increase of the ratio Fe to Mg in biotite (Fe-end member reactions), corresponding to the higher ratio Fe/Fe + Mg in biotite from the highest-temperature sillimanite zone 2 in comparison with lower-temperature zones (Tab. 3). The reactions (3) and (3') result in an increase of the ratio of Mg to Fe (Mg-end member reactions), corresponding to the composition of the studied garnets (Tab. 1). The composition of garnet and biotite in the sillimanite zone 2 could be as well affected by the different lithologic character and bulk composition of rocks with high Mn contents. The formation of garnet in the sillimanite zone 2 could take place in presence of biotite and sillimanite, according to the reaction:

$$\text{(Fe-Mg-Mn)biotite} + \text{sillimanite} = \text{(Fe-Mg-Mn)garnet} + \text{muscovite} \qquad (5)$$

leading to an increase of Mg and decrease of Mn in garnet during its progressive growth. The reaction (5) is supported also by the presence of biotite and sporadically of sillimanite inclusions in garnet, while staurolite inclusions have not been observed.

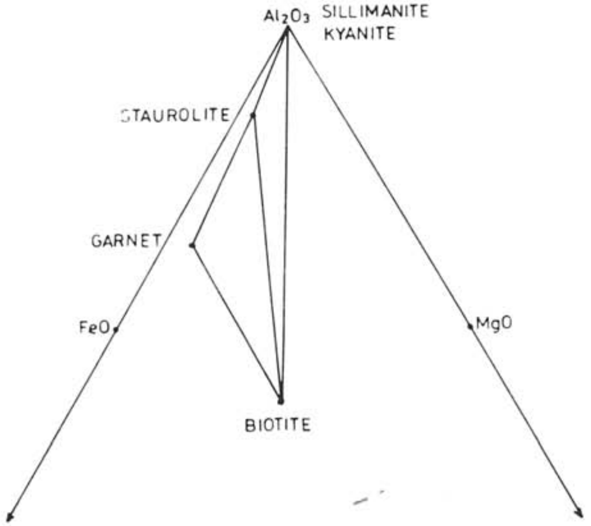

Fig. 11. AFM diagram (Thompson projection) expressing the observed mineral assemblages in the metapelites of the staurolite-kyanite-sillimanite zone. All assemblages include quartz, plagioclase, muscovite and ilmenite as well. The composition of minerals is based on microprobe analyses (Tabs. 1—5).

The changes in mineral assemblages as well as in the composition of the individual minerals during progressive metamorphism of the studied metapelites are shown on AFM diagrams in Thompson's projection (Thompson, 1957) (Figs. 11, 12, 13).

The formation of sillimanite due to kyanite breakdown by direct tranformation

$$\text{kyanite} = \text{sillimanite} \qquad (6)$$

has been observed only sporadically. Kyanite and sillimanite usually coexist without any mutual contact. The breakdown of kyanite and the formation of sillimanite could therefore take place by the mechanism of local ion-exchange reactions in different microscopic rock domains, between which elements were transported by diffusion in intergranular fluid due to chemical potential gradients (Carmichael, 1969; Eugster, 1970; Fisher, 1970). On the assumption of limited mobility of Al in the fluid, local reactions could take place in individual mineral assemblages with constant Al (Carmichael, 1969):

$$3 \text{ kyanite} + 3 \text{ quartz} + 2 K^+ + 3 H_2O = 2 \text{ muscovite} + 2 H^+ \quad (7)$$

$$4 \text{ kyanite} + 3 \text{ quartz} + 2 K^+ + 3 H_2O = 2 \text{ muscovite} + \text{sillimanite} + 2 H^+ \quad (8)$$

$$2 \text{ muscovite} + 2 H^+ = 3 \text{ sillimanite} + 3 \text{ quartz} + 2 K^+ + 3 H_2O \quad (9)$$

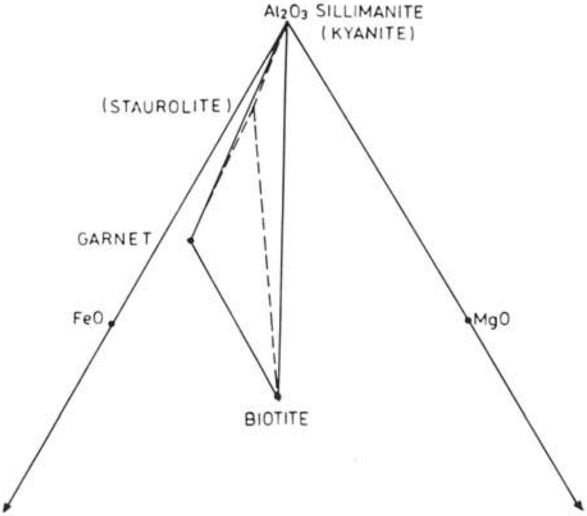

Fig. 12. Topology of discontinuous reaction (1) of staurolite breakdown on the isograd separating the staurolite-kyanite-sillimanite zone from the sillimanite zone 1, expressed in the diagram AFM (Thompson projection).

The abovementioned reactions can be applied in the interpretation of some of the observed microstructures, e.g. the reaction (7) is expressing the observed breakdown of kyanite and the formation of reaction rims of muscovite porphyroblasts on kyanite, the reaction (8) describes the formation of muscovite and sillimanite intergrowths surrounding the decomposing kyanite and the reaction (9) the formation of symplectites of sillimanite and quartz from muscovite. The reactions (7) + (9) and (8) + (9) occuring simultaneously result in the reaction (6) – kyanite = sillimanite.

Indirect reactions of the transformation of kyanite into sillimanite by the ion-exchange mechanism in the presence of fluid phase require lower activation energy and lower overstepping of equilibrium reaction temperature than the direct transformation with a small change of entropy (Carmichael, 1969; Walther–Wood, 1984). The coexistence of kyanite with sillimanite in the studied region in a relatively wide metamorphic zone could indicate a lower rate of metamorphic reactions, controlled especially by the rate of heat flow and by the diffusion transport of elements in intergranular fluid (e.g. Fisher, 1978; Walther–Wood, 1984; Rubie–Thompson, 1985).

Sillimanite could originate as a result of a similar reaction mechanism including other mineral phases, above all biotite, garnet and staurolite, as mentioned e.g. by Chinner (1961), Foster (1977) and Yardley (1977).

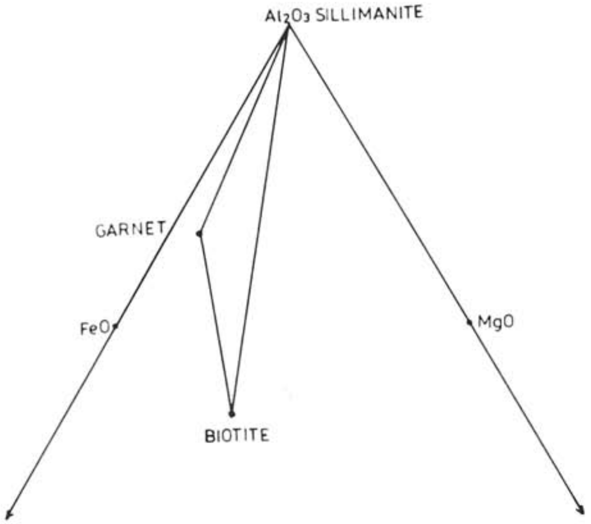

Fig. 13. Observed mineral assemblages in metapelites of the sillimanite zone 2 expressed in the diagram AFM (Thompson projection). All assemblages include quartz, plagioclase, muscovite and ilmenite. The composition of minerals is based on microprobe analyses (Tabs. 1—5).

The very often observed formation of sillimanite (fibrolite) from biotite could take place approximately according to the reaction:

$$\text{biotite} + H^{+} = \text{sillimanite} + K^{+} + (Mg, Fe)^{2+} + \text{quartz} + H_2O \qquad (10)$$

Complete substitution of biotite by sillimanite requires a contribution of Al from the breakdown of kyanite, staurolite and maybe garnet (Chinner, 1961; Foster, 1977; Yardley, 1977). K released by the biotite breakdown could participate in the formation of the "late" muscovite porphyroblasts and Mg, Fe and Ti could take part in the formation of opaque minerals, especially ilmenite; this is in accordance with the petrographic observations.

Kerrick (1987) describes the formation of fibrolite from biotite by the reaction (10) due to the activity of acid fluids released at the crystallization of granitoid intrusions in contact aureoles of Donegal. The formation of sillimanite (fibrolite) in the Western Tatra Mts. crystalline complexes occurred in the stability field of sillimanite and kyanite after Holdaway (1971) – Fig. 14. Sillimanite (fibrolite) was formed in zones of regional extent which are the result of progressive increase of metamorphic conditions, while sillimanite (fibrolite) occurs here frequently in a considerable distance from the granitoid intrusion.

P-T Conditions of metamorphism

Geothermometry and geobarometry

Temperature conditions of metamorphism have been calculated on the basis of the exchange reaction:

$$\text{Fe-garnet} + \text{Mg-biotite} = \text{Mg-garnet} + \text{Fe-biotite} \qquad (11)$$

using the garnet-biotite geothermometer of Ferry–Spear (1978), Perchuk et al. (1983) and Ganguly–Saxena (1984).

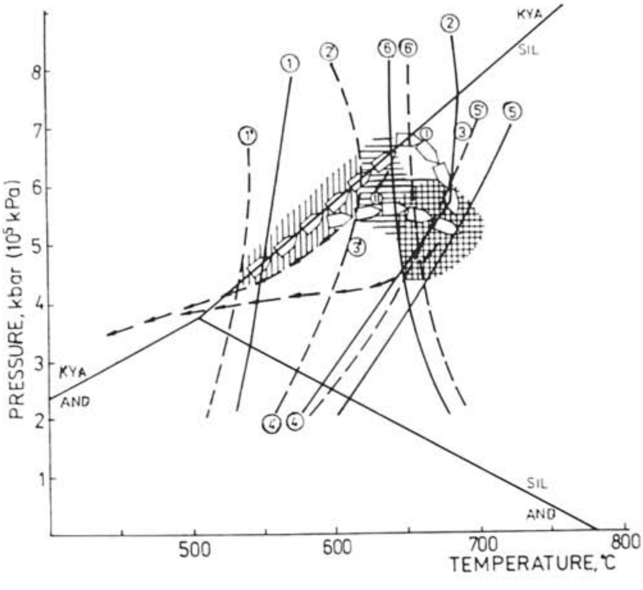

Fig. 14. Petrogenetic grid with assumed P-T paths of progressive metamorphism (thick arrows) and retrograde metamorphism (thin arrows) in the SW part of the Western Tatra Mts. crystalline complexes.

Explanations: Hatching marks stability fields of mineral assemblages in individual metamorphic zones on the basis of thermobarometric calculations and phase equilibria. Vertical hatching — staurolite-kyanite-sillimanite zone, horizontal hatching — sillimanite zone 1, cross-hatching — sillimanite zone 2. Experimentally determined stability curves with $X_{H_2O} = 1$ are marked by full line. 1 — chloritoid breakdown with the formation of staurolite (Ganguly, 1969; Hoschek, 1969); 2, 3, 4 — Fe-staurolite breakdown into sillimanite, kyanite and almandine (Richardson, 1968; Hoschek, 1969; Ganguly, 1972); 5 — breakdown of muscovite into K-feldspar (Kerrick, 1972); 6 — beginning of granite melting (Kerrick, 1972). Tripple point of Al_2SiO_5 polymorphs according to Holdaway (1971). Dashed line and marked by apostrophes — adjusted curves at the assumption of fluid composition with $X_{H_2O} = 0.8$.

On the basis of the study of garnet zoning it can be assumed that garnet core and biotite inclusions as well as garnet rim and biotite of matrix were during prograde metamorphism in equilibrium. Garnet rim was in some cases re-equilibrated with the coexisting biotite during cooling and retrograde metamorphism, so that peak metamorphic conditions corresponded to the temperatures calculated from the garnet core or garnet rim in a certain distance from the edge.

The geothermometer of Ferry–Spear (1978) is based on ideal mixing of Fe, Mg, Mn and Ca cations in garnet and it does not take into account the effects of Ca and Mn on the temperature. Ganguly–Saxena (1984) assume non-ideal mixing of all cations in garnet and they present corrections allowing for the effect of Ca and Mn in garnet on the temperature calculated according to Ferry–Spear (1978). We have therefore applied in our calculations of temperature the corrections for the effect of Ca and Mn, on the assumption of non-ideal mixing of all cations, with Margule's parameters W, after Ganguly–Saxena (1984, Tab. 2). The effect of Mn is considered also by Perchuk et al. (1983).

If we compare the temperatures calculated according to the above mentioned thermometers (Tab. 6), certain differences can be seen which are most pronounced at high temperatures. The effect of Ca and Mn calculated according to Ganguly–Saxena (1984) caused an increase in temperature values in comparison with the values according to Ferry–Spear (1978). Temperatures calculated according to Perchuk et al. (1983) in comparison with the values calculated according to Ferry and Spear (1978) are higher in the staurolite-kyanite-sillimanite zone and lower in the sillimanite zones 1 and 2. Most pronounced differences in temperatures are in the sillimanite zone 2 (as much as 100 °C), considerably exceeding the uncertainity of the garnet-biotite geothermometer, e.e. ± 25 to 50 °C.

Pressure has been calculated on the basis of the equlibrium reaction:

$$3 \text{ anorthite} = \text{grossular} + 2\ Al_2SiO_5 + \text{quartz} \qquad (12)$$

according to the calibration of Ghent et al. (1979), from the assemblage plagioclase-garnet-quartz-kyanite or sillimanite. Ghen et. al. (1979) considered also the activity of the grossular component in garnet and anorthite component in plagioclase by means of an introduction of the empirical activity coefficient K_γ (Tab. 6).

Temperatures and pressures calculated on the basis of a simultaneous solution of the equilibrium reactions (11) and (12) using the abovementioned garnet-biotite thermometers and garnet-plagioclase barometer are in Tab. 6. The calculated values of temperature and pressure correspond to the stability field of sillimanite, or they lie in the proximity of the equilibrium curve kyanite-sillimanite after Holdaway (1971), (Fig. 14).

Petrogenetic grid

Except data calculated on the basis of thermobarometry, petrogenetic grid of the stability of the observed mineral assemblages is usually used with the purpose of a more precise determination of P-T conditions of metamorphism (e.g. Thompson, 1976b; Korikovsky, 1979). For the determination of

Table 6

Temperatures (°C) and pressures (kbar, 10^5 kPa) calculated on the basis of garnet-biotite geothermometry and garnet-plagioclase geobarometry

sample	minerals	Gt-Bi $\ln K_D$*	Gt-Pl $\log K_D$**	P_G	T_{FS}	P_G	T_{GS}	P_G	T_P
		staurolite-kyanite-sillimanite zone							
17A	$^+Gt_{15r}Bi_{16}Pl_{21}$	1.804	— 2.806	3.8	549	4.2	568	4.0	557
17B	$Gt_{42r}Bi_{41}Pl_{34}$	1.926	— 2.715	3.4	510	3.8	531	3.8	535
18	$Gt_{20r}Bi_{23}Pl_{19}$	1.812	— 2.473	4.6	549	5.2	578	4.9	562
20	$Gt_{5r}Bi_{1}Pl_{21}$	1.743	— 2.195	5.9	577	6.3	606	5.9	584
		sillimanite zone 1							
74A	$Gt_{3r}Bi_{1}Pl_{5}$	1.546	— 2.708	5.5	646	5.6	656	5.9	616
74B	$Gt_{8r}Bi_{14}Pl_{6}$	1.607	— 2.454	5.9	625	6.3	646	5.7	613
96	$Gt_{7r}Bi_{3}Pl_{10}$	1.579	— 2.260	6.7	639	6.7	640	6.5	625
		sillimanite zone 2							
3	$Gt_{11c}Bi_{10in}Pl_{4}$	1.432	— 3.025	5.1	693	5.8	743	4.3	635
3	$Gt_{1r}Bi_{2}Pl_{4}$	1.463	— 3.058	4.7	677	5.6	732	3.8	629
5	$Gt_{19r}Bi_{21}Pl_{15}$	1.482	— 3.138	4.4	668	5.0	711	3.8	625
53	$Gt_{5r}Bi_{1}Pl_{15}$	1.471	— 2.847	5.5	677	6.1	720	4.8	632

$^+$ mineral analyses in Tables 1, 3 and 5;
P_G — pressures calculated according to Ghent et al. (1979);
T_{FS} — temperatures calculated according to Ferry-Spear (1978);
T_{GS} — Ganguly—Saxena (1984), T_P — Perchuk et al. (1983);
* $K_D = X_{Fe}^{Gt} \cdot X_{Mg}^{Bi} / X_{Fe}^{Bi} \cdot X_{Mg}^{Gt}$;
** $\log K_D = \log K_S + \log K_Y$, $K_S = X_{Gr}3/X_{An}3$, $\log K_Y = -0.4$ (Ghent et al. 1979).

P-T conditions of metamorphism in the Western Tatra Mts. crystalline complexes, stability curves of chloritoid, staurolite, kyanite, sillimanite, muscovite as well as of initial melting with the formation of minimum melt of granite composition are of critical importance.

The experimentally calibrated equilibrium curves (Fig. 14), at the assumed pressure $P_{fluid} = P_{H_2O} = P_{total}$ and fluid composition $X_{H_2O} = 1$, are not always in accordance with the stability of the observed mineral assemblages, nor with data of thermobarometry. This applies above all to the stability of staurolite, determined experimentally by Richardson (1968), Hoschek (1969) and Ganguly (1972), Fig. 14. On the basis of lithologic composition of metamorphites from the studied region and of data on the composition of metamorphic fluids (e.g. Ferry–Burt, 1982) it can be assumed that the composition of the fluids corresponded to a mixture of H_2O with smaller amounts above all of CO_2, CH_4, H_2S and chlorides. In the lithology of the SW part of the Western Tatry Mts. crystalline complexes predominant are metapelites with a little graphite admixture and metapsammites, metabasites occur in minor quantities and metacarbonates are absent altogether. According to the data of Ohmoto and Kerrick (1977), fluids in equilibrium with graphite have maximum $X_{H_2O} = 0.8–0.9$ at the temperatures 500–800 °C and pressures 4–7 kbar corresponding to the conditions in the studied region. Assuming that $P_{H_2O} < P_{fluid} = P_{total}$ and that the composition of fluid had maximum $X_{H_2O} = 0.8$, the stability curves of critical mineral assemblages have been adjusted for metamorphic conditions in the SW part of the Western Tatra Mts. crystalline complexes (Fig. 14). Curves at a lower X_{H_2O} decrease the temperature of metamorphic reactions and increase the temperature of initial melting so that they agree better with the P-T conditions calculated on the basis of thermobarometry and they are also in accordance with petrographic observations. On the basis of these data, breakdown of staurolite in association with kyanite, sillimanite and muscovite took place at a maximum temperature of approx. 600 °C; this corresponds also to the observations of Pigage and Greenwood (1982) concerning staurolite stability in a similar metamorphic assemblage and in P-T conditions quite different from the experimentally determined equilibria of Fe-staurolite.

For metapelites of the staurolite-kyanite-sillimanite zone, reasonable conditions of progressive metamorphism are the temperatures 530—600 °C and pressures 4—6.5 kbar, corresponding to the coexistence of staurolite with kyanite and sillimanite in the proximity of the curve kyanite-sillimanite confined by the stability curves of chloritoid and staurolite breakdown (Fig. 14). Lower temperatures correspond to the stability field of chloritoid formed in the process of retrograde metamorphism, as it has been indicated by petrographic observations.

P-T conditions attained in the sillimanite zone 1 correspond to the field confined by the curves of staurolite breakdown and the beginning of melting. Kyanite stability in this zone corresponds to the conditions near the equilibrium kyanite = sillimanite, or to the kyanite field. The temperature of progressive metamorphism reached in the sillimanite zone 1 approx. 600—650 °C at the pressure 5.5—7 kbar.

In the sillimanite zone 2, acceptable temperatures are 650—700 °C at pressures of 4.5—6 kbar which correspond to the conditions of high-grade metamorphism and are favourable for partial melting in the muscovite stability field, or near the univariant curve of muscovite breakdown with the formation of K-feldspar. In these P-T conditions and in the presence of a sufficient quantity of an H_2O-rich fluid phase, initial melting could occur even before the sillimanite-K--feldspar isograd was reached (e.g. Thompson—Tracy, 1977), and migmatites could be formed in which paleosome contains muscovite and K-feldspar is present in leucosome.

Discussion

The pathway of P-T conditions in the studied region of the SW part of the Western Tatra Mts. crystalline complexes is expressed by the P-T paths on Fig. 14. They correspond to the "peak", conditions deduced from the metamorphic zone sequence, thermobarometric data and from the stability of mineral assemblages in petrogenetic grid. They are expressing rather the course of metamorphic geotherm (England—Richardson, 1977) than P-T trends of individual rocks which can be deduced from a detailed study of zonal minerals, especially garnet, e.g. Spear—Selverstone (1983), Thompson—England (1984).

The P-T path I of progressive metamorphism (Fig. 14) is expressing the temperature and pressure increase at the transition from the staurolite-kyanite-sillimanite zone to the area of kyanite and sillimanite stability after staurolite breakdown in the sillimanite zone 1 where maximum pressure conditions were reached. The transition into the area of the sillimanite zone 2 occurred at a further temperature increase, but a decrease of pressure. Peak temperature was reached in the conditions of partial melting enabling the formation of migmatites. The increase of temperature with a certain decrease of pressure could be caused by thermal decompression (England–Thompson, 1984) which was probably connected with temperature increase during uplift and erosion, or with gravitational instability of the rising granitoid melt (England–Richardson, 1977; England–Thompson, 1984), while the uplift could start already before peak metamorphic temperatures were reached and before the granitoid intrusion. The trend I also gives the possibility of the formation of granite-gneisses at pressures of 6–7 kbar and temperature over 650 °C, with sufficient quantity of H_2O, before the intrusion of the main granitoid body.

The path II (Fig. 14) is expressing the transition from the staurolite-kyanite-sillimanite zone into the sillimanite zones 1 and 2, with an approximately simultaneous breakdown of staurolite and sillimanite, as it was observed on some locations in field, e.g. in the Jalovecká Valley. This path shows the temperature increase at a slight pressure decrease in approximately the same depth level.

Granitoid magmatism, according to geochronological data, was practically synchronal with or followed immediately after the culmination of regional metamorphism and in relation to metamorphic structures it had mostly late-tectonic character of emplacement. An increased heat flow in connection with the granitoid magmatism probably influenced the course of metamorphic geotherm, while the highest-temperature metamorphic zone — the sillimanite zone 2 — surrounds the granitoid body. A contact-thermal effect of the granitoids on the surrounding rocks which would cause formation of contact hornfelses has not been observed. From the results of the study of P-T conditions of metamorphism it follows that gneisses and migmatites on the contact with granitoids were formed in the conditions of temperatures over 650 °C and pressures of approx. 5 kbar corresponding to the conditions of high-grade medium-pressure kyanite-sillimanite type of regional metamorphism. The present position of the granitoids, together with migmatites and gneisses of the highest-temperature sillimanite zone 2, on metamorphites of lower-temperature zones, proved on many locations to be tectonic (Kahan, 1969), indicates as well tectonic influence on the original course of the metamorphic zones and on the position of granitoids.

Retrograde processes connected with a more extensive effect of fluids and with tectonic deformations could take place after peak conditions of progressive metamorphism were reached, at lower temperatures in the last stages of the Hercynian metamorphic cycle. Suggested trends of retrograde metamorphism are on Fig. 14.

Conclusions

Metamorphism in the SW part of the Western Tatra Mts. crystalline complexes had zonal character and its result was the formation of staurolite-kyanite-sillimanite zone and sillimanite zone divided into two subzones, 1 and 2, which are expressing the increase of metamorphic conditions, most probably in the Hercynian cycle.

The distribution of metamorphic zones in space was affected by the original development of the metamorphic geotherm and by the temperature increase from SW to NE, mostly in the direction towards the granitoid body, but as well by tectonics, especially by the thrusting of the migmatite complex with the granitoids on the metamorphic complex along a flat diaphtorite-phyllonite fault. The thrusted complex corresponds mostly to the higher-temperature part of the sillimanite zone and the basement complex to its lower-temperature part with the staurolite-kyanite-sillimanite zone.

The transition from the staurolite-kyanite-sillimanite zone into the sillimanite zone is expressed by an isograd based on the breakdown of staurolite and the formation of sillimanite. Kyanite remains stabile in many places even after the staurolite breakdown in the lower-temperature part of the sillimanite zone, where it coexists with fibrolitic sillimanite. Kyanite and sillimanite are coexisting in P-T conditions corresponding to their stability near the kyanite-sillimanite stability curve after Holdaway (1971), or they are metastable in a cerinterval overstepping the equilibrium temperature-pressure conditions near the univariant curve. Direct transformation of kyanite to sillimanite is rare and sillimanite was usually formed by indirect breakdown of kyanite as well as by the breakdown of biotite, staurolite, garnet and muscovite. The rate of the metamorphic reactions was controlled above all by heat flow and diffusion.

P-T conditions of metamorphism have been determined on the basis of thermobarometric calculations and petrogenetic grid. The temperature of progressive metamorphism in the staurolite-kyanite-sillimanite zone reached approximately 530—600 °C at a pressure of 4—6.5 kbar. In the sillimanite zone 1, the temperature reached 600—650 °C and the pressure 5.5—7 kbar. In the sillimanite zone 2 peak temperatures were 650—700 °C at the pressure 4.5—6 kbar; in these conditions with a sufficient quantity of H_2O-rich fluid phase, initial melting and migmatite formation could take place. The assumed composition of the fluid phase corresponded to $X_{H_2O} \approx 0.8$, while $P_{H_2O} < P_{fluid} = P_{total}$.

Relatively extensive retrograde metamorphism, connected with the effect of fluids in lower P-T conditions, caused the formation of above all chloritoid, chlorite and white micas — muscovite and margarite — in the metapelites.

The P-T paths of metamorphic conditions evolution correspond to an increase of temperature and pressure before the culmination of metamorphism. In the last stages of progressive metamorphism, at the maximum temperature increase, certain pressure decrease took place which could be connected with uplift and erosion and as well with granitod magmatism. Progressive metamorphism in the SW part of the Western Tatra Mts. crystalline complexes corresponded to the medium-pressure kyanite-sillimanite type of regional metamorphism facies series.

Translated by K. Janáková

REFERENCES

ALBEE, A. L. — CHODOS, A. A., 1969: Minor element content of coexistent Al_2SiO_5 polymorphs. Amer. J. Sci. (New Haven), 267, pp. 310—316.

ALBEE, A. L. — RAY, L., 1970: Correction factors for electron probe micro-analysis of silicates, oxides, carbonates, pfosphates, and sulfates. Analyt. Chem. 42, pp. 1408—1414.

BENCE, A. E. — ALBEE, A. L., 1968: Empirical correction factors for the electron microanalysis of silicates and oxides. J. Geol. (Chicago), 76, pp. 382—403.
BURCHART, J., 1968: Rubidium-Strontium isochron ages of the crystalline core of the Tatra mountains, Poland. Amer. J. Sci. (New Haven), 266, pp. 895—907.
BURCHAR,T J., 1970: Skaly krysztaliczne wyspy Goryczkowej w Tatrach. Stud. geol. Pol. (Warszawa), 32, pp. 7—183.
CAMBEL, B. — SHCHERBAK, N. P. — KAMENICKÝ, L. — BARTNITSKII, E. N. — VESELSKY, J., 1977: Nekatorie svedenia po geokhronologii kristalinikuma Zapadnikh Karpat na osnove dannykh U-Th-Pb metoda. Geol. Zbor. Geol. carpath. (Bratislava), 28, 2, pp. 243—259.
CARMICHAEL, D. M., 1969: On the mechanism of prograde metamorphic reactions in quartz-bearing pelitic rocks. Contr. Mineral. Petrology (Berlin—New York), 20, pp. 244—267.
CARMICHAEL, D. M., 1970: Intersecting isograds in the Whetstone lake area, Ontario. J. Petrology (Oxford), 11, pp. 147—181.
CHINNER, G. A. 1961: The origin of sillimanite in Glen Clova, Angus. J. Petrology (Oxford), 2, pp. 312—323.
ENGLAND, P. C. — RICHARDSON, S. W., 1977: The influence of erosion upon the mineral facies of rocks from different metamorphic environments. J. geol. Soc. (London), 134, pp. 201—213.
ENGLAND, P. C. — THOMPSON, A. B., 1984: Pressure-temperature-time paths of regional metamorphism I. Heat transfer during the evolution of regions of thickened continental crust. J. Petrology (Oxford), 25, pp. 894—928.
EUGSTER, H. P., 1970: Thermal and ionic equilibria among muscovite, K-feldspar and alumosilicate assemblages. Fortschr. Miner. (Stuttgart), 47, pp. 106—123.
EVANS, B. W. — GUIDOTTI, C. V., 1966: The sillimanite-potash feldspar isograd in western Maine, U.S.A. Contr. Mineral. Petrology (Berlin—New York), 12, pp. 25—62.
FERRY, J. M. — BURT, D. M., 1982: Characterization of metamorphic fluid composition through mineral equilibria. In: Characterization of metamorphism through mineral equilibria. J. M. Ferry (ed.). Reviews in Mineralogy, 10, pp. 207—262.
FERRY, J. M. — SPEAR, F. S., 1978: Experimental calibration of the partitioning of Fe and Mg between biotite and garnet. Contr. Mineral. Petrology (Berlin—New York), 66, pp. 113—117.
FISHER, G. W., 1970: The application of ionic equilibria to metamorphic differentation: an example. Contr. Mineral. Petrology (Berlin—New York), 29, pp. 91—103.
FISHER, G. W., 1978: Rate laws in metamorphism. Geochim. Cosmochim. Acta (Oxford), 42, pp. 1035—1050.
FOSTER, C. T. Jr., 1977: Mass transfer in sillimanite-bearing pelitic schists near Rangeley, Maine. Amer. Mineralogist (Washington), 62, pp. 727—746.
GANGULY, J., 1969: Chloritoid stability and related parageneses: theory, experiments, and applications. Amer. J. Sci. (New Haven), 267, pp. 910—944.
GANGULY, J., 1972: Staurolite stability and related parageneses: theory, experiments, and applications. J. Petrology (Oxford), 13, pp. 335—365.
GANGULY, J. — SAXENA, S. K, 1984: Mixing properties of aluminosilicate garnets: constraints from natural and experimental data, and applications to geothermo--barometry. Amer. Mineralogist (Washington), 69, pp. 88—97.
GHENT, E. D. — ROBBINS, D. S. — STOUT, M. Z., 1979: Geothermometry, geobarometry, and fluid compositions of metamorphosed calc-silicates and pelites, Mica Creek, British Columbia. Amer. Mineralogist (Washington), 64, pp. 874—885.
GOREK, A., 1956: Geologická stavba Západných Tatier. Geol. Sbor. (Bratislava), 7, pp. 1—2.
GOREK, A., 1959: Prehľad geologických a petrografických pomerov kryštalinika Vysokých Tatier. Geol. Sbor. (Bratislava), 10, 1, pp. 13—88.
GOREK, A., 1967: Povaha poruchových pásiem v kryštaliniku Vysokých Tatier a ich odraz v tektonickom vývoji mezozoických sérií. Acta geol. geogr. Univ. Comen., Geol. (Bratislava), 12, pp. 5—12.
GOREK, A., 1969: Postavenie zvyškov metamorfovaného plášťa v granitoidnom masíve Vysokých Tatier a ich vzťah ku kryštalickým bridliciam a migmatitom v Západných Tatrách. Acta geol. geogr. Univ. Comen., Geol. (Bratislava), 18, pp. 103—116.

GRAMBLING, J. A. — WILLIAMS, M. L., 1985: The effects of Fe^{3+} and Mn^{3+} on aluminum silicate phase relations in north-central New Mexico, U.S.A. J. Petrology (Oxford), 26, pp. 324—354.

GUIDOTTI, C. V., 1970: The mineralogy and petrology of the transition from the lower to upper sillimanite zone in the Oquossoc area, Maine. J. Petrology (Oxford), 11, pp. 277—336.

GUIDOTTI, C. V., 1984: Micas in metamorphic rocks. In: Micas. Rewievs in Mineralogy, 13, pp. 357—468.

HOLDAWAY, M. J., 1971: Stability of andalusite and the aluminum silicate phase diagram. Amer. J. Sci. (New Haven), 271, pp. 97—131.

HOSCHEK, G., 1969: The stability of staurolite and chloritoid and their significance in metamorphism of pelitic rocks. Contr. Mineral Petrology (Berlin—New York), 22, pp. 208—232.

JAROSZEWSKI, W., 1965: Budowa geologiczna gornej czesci doliny Koščieliskiej w Tatrach. Acta Geol. Pol. (Warszawa), 15, pp. 429—496.

JOHANNES, W., 1983: On the origin of layered migmatites. In: Migmatites, melting and metamorphism. Atherton, M. P. and Gibble, C. D. (eds.). Shiva, Nantwich, pp. 235—248.

KAHAN, Š., 1967: Príspevok k litológii kryštalických bridlíc v Západných Tatrách. Acta geol. geogr. Univ. Comen., Geol. (Bratislava), 12, pp. 47—62.

KAHAN, Š., 1968: K problematike vystupovania staurolitu, disténu, sillimanitu a korundu v kryštaliniku Západných Tatier. Acta geol. geogr. Univ. Comen., Geol. (Bratislava), 13, pp. 191—202.

KAHAN, Š., 1969: Eine neue ansicht über den geologischen aufbau des kristallinikums der West-Tatra. Acta geol. geogr. Univ. Comen., Geol. (Bratislava), 18, pp. 19—78.

KAHAN, Š. — HVOŽDARA, P., 1967: Distén — nový minerál v kryštaliniku Vysokých Tatier. Acta geol. geogr. Univ. Comen., Geol. (Bratislava), 12, pp. 115—122.

KANTOR, J., 1959: Vek niektorých vysokotatranských granitoidov a kryštalických bridlíc rádioaktívneho rozpadu K^{40}. Geol. Sbor. (Bratislava), 10, pp. 89—96.

KERRICK, D. M., 1972: Experimental determination of muscovite + quartz stability with $P_{H_2O} < P_{total}$. Amer. J. Sci. (New Haven), 272, pp. 946—958.

KERRICK, D. M., 1987: Fibrolite in contact aureoles of Donegal, Ireland. Amer. Mineralogist (Washington), 72, pp. 240—254.

KORIKOVSKY, S. P., 1979: Fatsii metamorfizma metapelitov. Nauka, Moskva, 262 pp.

KOUTEK, J., 1935: O krystalických břidlicích skupiny Barance (2181 m) v Liptovských Holích. Věst. St. geol. Úst. (Praha), 11, pp. 8—14.

MEHNERT, K. R., 1968: Migmatites and the origin of granitic rocks. Elsevier, Amsterdam, 405 pp.

OHMOTO, H. — KERRICK, D. M., 1977: Devolatilization equilibria in graphitic systems. Amer. J. Sci. (New Haven), 277, pp. 1013—1044.

PERCHUK, L. L. — LAVRENTIEVA, I. V. — ARANOVICH, L. J. — PODLESSKII, K. K., 1983: Biotit-granat-kordieritovie ravnovesia i evolutsya metamorfizma. Nauka, Moskva, pp. 198.

PIGAGE, L. C. — GREENWOOD, H. J., 1982: Internally consistent estimates of pressure and temperature: The staurolite problem. Amer. J. Sci. (New Haven), 282, pp. 943—969.

RICHARDSON, S. W., 1968: Staurolite stability in a part of the system Fe-Al-Si-O-H. J. Petrology (Oxford), 9, 757—768.

RUBIE, D. C. — THOMPSON, A. B., 1985: Kinetics of metamorphic reactions at elevated temperatures and pressures: An appraisal of available experimental data. In: Metamorphic reactions: kinetics, textures and deformation. A. B. Thompson — D. C. Rubie (eds.). Advances in physical geochemistry, 4, Springer, New York, pp. 27—79.

SKUPIŇSKI, A., 1975: Petrogeneza i struktura trzonu krystalicznego Tatr Zachodnich miedzy Ornakiem i Rohaczami. Stud. geol. Pol. (Warszawa), 49, pp. 7—105.

SPEAR, F. S. — SELVERSTONE, J., 1983: Quantitative P-T paths from zoned minerals: theory and tectonic applications. Contr. Mineral. Petrology (Berlin—New York), 83, pp. 348—357.

THOMPSON, A. B., 1976a: Mineral reactions in pelitic rocks: I. prediction of P—T—X (Fe—Mg) phase relations. Amer. J. Sci. (New Haven), 276, pp. 401—424.

THOMPSON, A. B., 1976b: Mineral reactions in pelitic rocks: II. calculation of some P-T-X(Fe-Mg) phase relations. Amer. J. Sci. (New Haven), 276, pp. 425—454.

THOMPSON, A. B. — ENGLAND, P. C., 1984: Pressure-temperature-time paths of regional metamorphism II. Their inference and interpretation using mineral assemblages in metamorphic rocks. J. Petrology (Oxford), 25, pp. 929—955.

THOMPSON, A. B. — TRACY, R. J., 1979: Model systems for anatexis of pelitic rocks. II. Facies series melting and reactions in the system $CaO—KAlO_2—NaAlO_2—Al_2O_3—SiO_2—H_2O$. Contr. Mineral. Petrology (Berlin—New York), 70, pp. 429—438.

THOMPSON, J. B., Jr., 1957: The graphical analysis of mineral assemblages in pelitic schists. Amer. Mineralogist (Washington), 42, pp. 842—858.

TRACY, R. J., 1978: High grade metamorphic reactions and partial melting in pelitic schists, west-central Massachusetts. Amer. J. Sci. (New Haven), 278, pp. 150—178.

TRACY, R. J., 1982: Compositional zoning and inclusions in metamorphic minerals. In: Characterization of metamorphism through mineral equilibria. J. M. Ferry (ed.). Reviews in mineralogy, 10, pp. 355—397.

WALTHER, J. V. — WOOD, B. J., 1984: Rate and mechanism in prograde metamorphism. Contr. Mineral. Petrology (Berlin—New York), 88, pp. 246—259.

YARDLEY, B. W. D., 1977: The nature and significance of the mechanism of sillimanite growth in the Connemara schists, Ireland. Contr. Mineral. Petrology (Berlin—New York), 65, pp. 53—58.

Manuscript received November 4, 1987.